Biophysical Chemistry 193–194 (2014) 35–49

Contents lists available at ScienceDirect

Biophysical Chemistry

journal homepage: http://www.elsevier.com/locate/biophyschem

Calcium-dependent energetics of calmodulin domain interactions with regulatory regions of the Ryanodine Receptor Type 1 (RyR1)☆

Rhonda A. Newman [a,1], Brenda R. Sorensen [a], Adina M. Kilpatrick [b], Madeline A. Shea [a,*]

[a] Dept. of Biochemistry, Univ. of Iowa Roy J. and Lucille A. Carver College of Medicine, Iowa City, IA 52242-1109, United States
[b] Department of Physics and Astronomy, Drake University, Des Moines, IA 50311-4516, United States

HIGHLIGHTS

- Calcium-dependent energies of calmodulin domains binding to RyR1 sites were compared.
- CaM domains N and C bind preferentially to $RyR1_{3614–3643}$ rather than $RyR1_{1975–1999}$.
- $RyR1_{3614–3643}$ binds $(Ca^{2+})_2$–CaM_C ~5 kcal/mol more favorably than it binds apo CaM_C.
- CaM_N requires Ca^{2+} to bind RyR1 sites and is ~3.5 kcal/mol less favorable than CaM_C.
- CaM associated with $RyR1_{3614–43}$ retains sequential binding of Ca^{2+} to its domains.

GRAPHICAL ABSTRACT

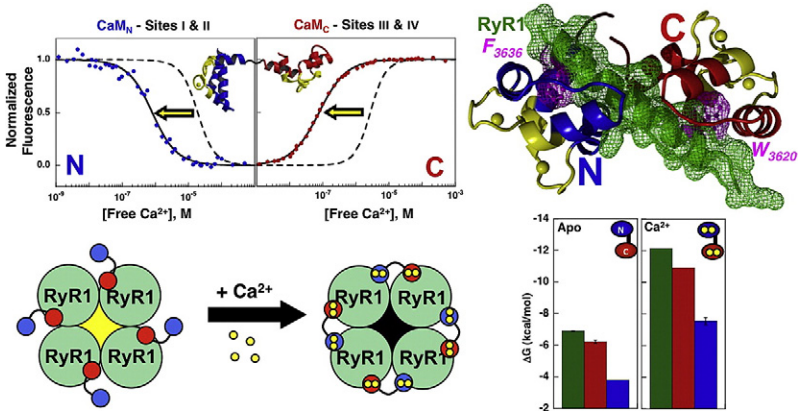

ARTICLE INFO

Article history:
Received 1 July 2014
Received in revised form 21 July 2014
Accepted 22 July 2014
Available online 30 July 2014

Keywords:
Fluorescence
Anisotropy

ABSTRACT

Calmodulin (CaM) allosterically regulates the homo-tetrameric human Ryanodine Receptor Type 1 (hRyR1): apo CaM activates the channel, while $(Ca^{2+})_4$–CaM inhibits it. CaM-binding RyR1 residues 1975–1999 and 3614–3643 were proposed to allow CaM to bridge adjacent RyR1 subunits. Fluorescence anisotropy titrations monitored the binding of CaM and its domains to peptides encompassing $hRyR_{11975–1999}$ or $hRyR1_{3614–3643}$. Both CaM and its C-domain associated in a calcium-independent manner with $hRyR1_{3614–3643}$ while N-domain required calcium and bound ~250-fold more weakly. Association with $hRyR1_{11975–1999}$ was weak. Both hRyR1 peptides increased the calcium-binding affinity of both CaM domains, while maintaining differences between them. These energetics support the CaM C-domain association with $hRyR1_{3614–3643}$ at low calcium, positioning CaM to

Abbreviations: λ_{em}, Emission wavelength; λ_{ex}, Excitation wavelength; BAA, Basic Amphipathic α-helix; $CaM_{1–148}$, Full-length calmodulin, encompassing residues 1 to 148; $CaM_{1–80}$, CaM N-domain encompassing residues 1 to 80; $CaM_{76–148}$, CaM C-domain, encompassing residues 76 to 148; Fl-hRyR1(1975–1999)p, hRyR1(1975–1999)p with a 5,6-carboxyfluorescein moiety at the N-terminus; Fl-hRyR1(3614–3643)p, hRyR1(3614–3643)p with a 5,6-carboxyfluorescein moiety at the N-terminus; hRyR1(1975–1999)p, Synthetic peptide representing amino acids 1975 to 1999 of the human Ryanodine Receptor Type 1; hRyR1(3614–3643)p, Synthetic peptide representing amino acids 3614 to 3643 of the human Ryanodine Receptor Type 1; NMDA, N-methyl D-aspartate; NTA, Nitrilotriacetic acid; Phe, phenylalanine; RyR1, Ryanodine Receptor Type 1; SK, small conductance potassium channel; Tyr, tyrosine; WT, wild-type.

☆ This study was supported by a University of Iowa Center for Biocatalysis and Bioprocessing NIH Biotechnology Training grant (NIH T32 GM08365) to R.A.N., a University of Iowa Carver College of Medicine FUTURE in Biomedicine Fellowship to A.M.K. and a grant from the National Institutes of Health (R01 GM 57001) to M.A.S.

* Corresponding author at: 51 Newton Rd., 4-411 BSB, Iowa City, IA 52242-1109, United States. Tel.: +1 319 335 7885; fax: +1 319 335 9570.
E-mail address: madeline-shea@uiowa.edu (M.A. Shea).
[1] Present address: Life Technologies, Frederick, MD, United States.

http://dx.doi.org/10.1016/j.bpc.2014.07.004

Titration
Intracellular calcium channel
Thermodynamics

respond to calcium efflux. However, the CaM N-domain affinity for $hRyR_{11975–1999}$ alone was insufficient to support CaM bridging adjacent RyR1 subunits. Other proteins or elements of the hRyR1 structure must contribute to the energetics of CaM-mediated regulation.

1. Introduction

Intracellular calcium fluxes play a major role in regulating vital cellular processes such as synaptic transmission, cell cycle progression, fertilization, and muscle contraction. It is necessary to regulate intracellular calcium levels to prevent prolonged exposure of cells to toxic levels of this ion. The essential calcium sensor calmodulin (CaM) is a central mediator of most calcium-signaling events [1]. This small (148 amino acids), acidic (pI ~ 4) protein contains two globular domains that share a common flexible linker region [2]. Each domain can bind two calcium ions cooperatively via two EF-hand calcium-binding motifs. The CaM N-domain (residues 1–80) contains calcium-binding sites I and II and the C-domain (residues 76–148) contains calcium-binding sites III and IV (Fig. 1A). Whereas the two domains share a high degree of similarity at both the sequence and structural levels, the C-domain coordinates calcium ions with a 10-fold higher intrinsic affinity than the N-domain [3–6].

In a classical model of CaM–target interactions, methionine-rich hydrophobic clefts in CaM that are exposed upon calcium binding allow CaM to bind a variety of target proteins including enzymes, cytoskeletal molecules, and ion channels with high affinity (K_d of 10^{-7} to 10^{-11} M) [1,7,8]. Whereas the binding of CaM to many of its targets depends upon saturation by calcium, some interactions are calcium-independent [9–12], while in others they depend on partial saturation of CaM with calcium. For example, in the cases of the Anthrax Edema Factor (Fig. 1E) and the small conductance potassium (SK) channel (Fig. 1F), one domain is calcium-saturated and the other is calcium-free (apo) [13,14].

Ryanodine Receptor Type 1 (RyR1) is the predominant intracellular calcium release channel in skeletal muscle. This large (~2.3 MDa) homo-tetrameric ion channel gates calcium efflux from the sarcoplasmic reticulum to the cytosol of the muscle cell. The cytoplasmic face of RyR1 constitutes more than 80% of the channel and is the site of allosteric regulation by endogenous cytosolic modulators such as CaM. Biochemical studies and cryo-EM three-dimensional reconstructions have shown that CaM binds to full-length RyR1 with nanomolar affinity both in the absence and presence of calcium, at a stoichiometry of one CaM molecule per RyR1 monomer [15–17]. CaM is a weak activator of RyR1 at submicromolar calcium levels and an inhibitor of the channel at micromolar calcium concentrations [18]. Essentially, CaM acts as a ligand-induced allosteric effector, which undergoes a calcium-dependent conformational change that, in turn, triggers a change in RyR1 to regulate its activity.

Previous studies have shown that both apo and calcium-saturated CaM associate with a region of mammalian RyR1 that maps to amino acids 3614 to 3643, and have reported that CaM binds a peptide corresponding to this region with similar affinity as it binds the full-length channel, both in the presence and the absence of calcium [15,16]. This sequence is highly-conserved across vertebrate ryanodine receptors, and has been defined as a novel '1–17' basic amphipathic alpha helix (BAA) motif in which W3620 and F3636 serve as hydrophobic anchors interacting with calcium-saturated CaM (Fig. 1B) [19]. Few structural contacts were observed between the N- and C-domains of calcium-saturated CaM in complex with residues 3614–3643, allowing for motions of the two domains while bound to the ryanodine receptor target [19,20]. Studies with synthetic peptides corresponding to nested sequences within RyR1(3614–3643) show that the C-terminal portion (residues 3635–3643) is required for apo CaM binding, while the N-terminal portion (residues 3614–3634) is necessary for calcium–CaM binding [16]. Additional data indicate that the residue-specific interactions between CaM and the 3614–3643 sequence are different in low versus high calcium environments. Alkylation of C3635 blocks apo CaM binding, but has no effect on the binding of calcium-saturated CaM [21]. Moreover, point mutations within the 3614–3643 region differentially affect channel regulation by apo or calcium-bound CaM [22–24]. Lastly, cryo-EM reconstructions of full-length RyR1 channels show that the apo and Ca^{2+}–CaM binding sites on the receptor are clearly distinct, albeit partially overlapping [17,25].

Binding studies with the individual domains of CaM reveal interesting insights into the functional and structural interplay of these domains when bound to RyR1. Models by Hamilton and colleagues proposed a calcium-independent binding of the CaM C-domain to the C-terminal region of RyR1(3614–3643) and its subsequent calcium-dependent translocation towards residue 3614 [26]. The CaM N-domain can bind to the C-terminal region of this sequence under calcium-saturating conditions, in what appears to be a low affinity interaction [26]. However, alkylation, crosslinking and tryptic cleavage studies [27] indicate that the N-domain can associate with a non-canonical CaM-binding motif (residues 1975–1999) located on an adjacent subunit that lies in close spatial proximity to residues 3614–3643, suggesting that CaM may bridge the RyR1(3614–3643) and RyR1(1975–1999) regions on neighboring RyR1 subunits. While a previous study has shown that association of CaM domains with the 3614–3643 CaM-binding motif is sufficient to explain the ability of CaM to regulate RyR1 activity, [28] the role of the CaM domains in the association with the 1975–1999 site has not yet been investigated.

The study presented here compares the energetics of calcium-dependent association between the CaM domains and two peptides corresponding to the 1975–1999 and 3614–3643 regions of human RyR1 (hRyR1(1975–1999)p and hRyR1(3614–3643)p, Fig. 1C and D), and the effect of this association on the energetics of calcium binding to the CaM domains. Our results confirm the calcium-independent association of the CaM C-domain to RyR1(3614–3643) observed previously [26], and are consistent with structural domain independence in the complex [19,20]. Association of CaM with RyR1(1975–1999) was calcium-dependent, physiologically relevant, and significantly weaker than that observed for RyR1(3614–3643).

Interaction of CaM with these regions increases the calcium-binding affinities of both the N- and C-domains of CaM, allowing CaM to regulate RyR1 channel activity over the physiological range of calcium concentrations during muscle contraction. Together, our results support a model of RyR1 regulation by CaM in which (a) the CaM C-domain binds to RyR1(3614–3643) under resting (apo or very low calcium) conditions, positioning CaM to respond to local changes in calcium concentration, and (b) calcium triggers a change in the CaM N-domain that allows it to associate with either of the two CaM-binding motifs (3614–3643 or 1975–1999). This is the first time that the domain-specificity of CaM interaction with the 1975–1999 CaM-binding region and corresponding changes in calcium-binding affinity have been explored, and our results contribute to our overall understanding of allosteric regulation of RyR1 via calcium-dependent regulation of CaM domains.

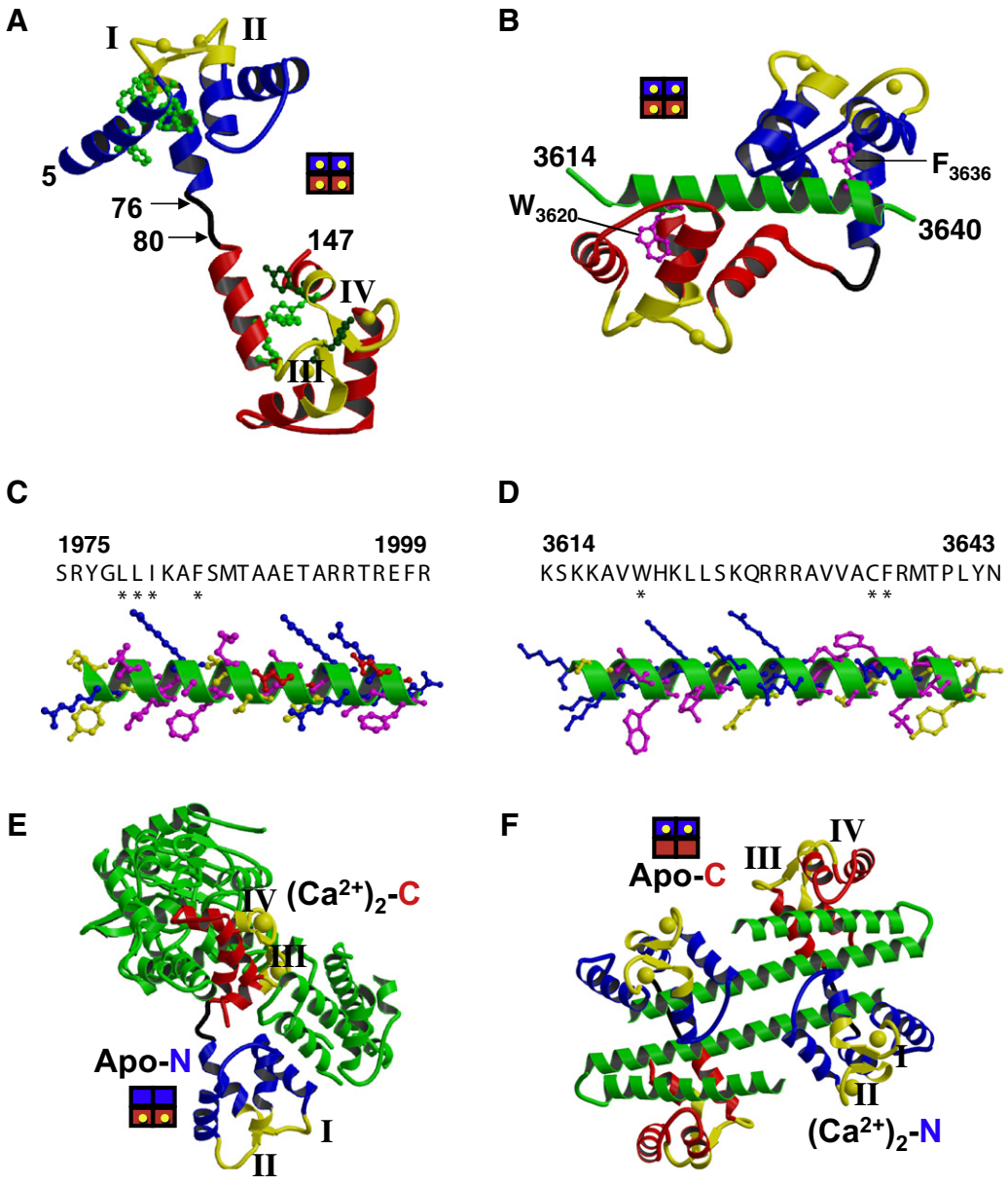

Fig. 1. Ribbon diagrams of CaM and CaM-binding motifs from the Human Ryanodine Receptor Type 1. These figures were created using SYBYL (MIPS3-IRIX 6.2 Tripos Associates Inc.), MOLSCRIPT [75] and RASTER3D [76]. The CaM N-domain (blue, residues 1–80) and the C-domain (red, residues 76–148) are connected by a flexible linker (black; residues 76 to 80). Calcium-binding sites (I, II, III, and IV) and calcium ions are highlighted in yellow, and target proteins/peptides are shown in green. Boxes illustrating the ligation state of CaM are included for ease of visualization. A. Ribbon diagram of calcium-saturated CaM_{1-148} (3CLN.pdb) [77] depicting the intrinsic fluorophores (green ball-and-stick) of the two CaM domains. B. Ribbon diagram of calcium-saturated CaM bound to RyR1(3614–3643)p (2BCX.pdb) [19]; hydrophobic anchor residues in RyR1 peptide, shown in magenta ball-and-stick. Residues 41–43 of the peptide were not defined. Sequence and helical model representations of CaM-binding domains of the human Ryanodine Receptor Type 1: C. hRyR1(1975–1999)p and D. hRyR1(3614–3643)p. Side-chains of hydrophobic (magenta), basic (blue), and hydrophilic (yellow) residues are shown in ball-and-stick. Asterisks below the sequences highlight the positions of residues that are proposed (in the case of hRyR1(1975–1999)p, panel C) or shown (in the case of hRyR1(3614–3643)p, panel D) to serve as hydrophobic anchor residues. E. Diagram of $(Ca^{2+})_2$–CaM (apo N-domain) in the presence of the Anthrax Edema Factor + 3D-ATP (1K90.pdb) [13]. F. Diagram of 2 $(Ca^{2+})_2$–CaM (apo C-domain) in the presence of 2 CaM binding peptides from the small conductance potassium (SK) channel (1G4Y.pdb) [14].

2. Materials and methods

2.1. Expression and purification of WT CaM

The pET vectors for over-expression of the full-length mammalian CaM (CaM_{1-148}) and the corresponding domain fragments (CaM_{1-80} and CaM_{76-148}) were described previously [29–32]. Recombinant CaM proteins were purified on phenyl sepharose CL-4B columns [33]. To precipitate contaminating proteins with a lower thermal stability than calcium-saturated CaM, eluate was incubated at 80 °C for 10 min in the presence of 10 mM $CaCl_2$ (total) before it was purified on a phenyl sepharose column pre-equilibrated with $CaCl_2$-containing buffer. In some instances, the proteins required further purification via DEAE-Sephacel anion exchange and/or HiLoad 26/60 Superdex 75 (GE Healthcare) chromatography. The purified recombinant proteins were shown to be 95–99% pure, as judged by reversed-phase HPLC. Protein

concentrations were determined by UV absorbance in the presence of 0.1 N NaOH, using published extinction coefficients for Phe and Tyr [34] (CaM does not contain Trp).

2.2. Preparation of hRyR1 peptides

Peptides corresponding to the 1975–1999 and 3614–3643 regions of human RyR1—hRyR1(1975–1999)p (Acetyl-Ser-Arg-Tyr-Gly-Leu-Leu-Ile-Lys-Ala-Phe-Ser-Met-Thr-Ala-Ala-Glu-Thr-Ala-Arg-Arg-Thr-Arg-Glu-Phe-Arg-NH_2) and hRyR1(3614–3643) (Acetyl-Lys-Ser-Lys-Lys-Ala-Val-Trp-His-Lys-Leu-Leu-Ser-Lys-Gln-Arg-Arg-Arg-Ala-Val-Val-Ala-Cys-Phe-Arg-Met-Thr-Pro-Leu-Tyr-Asn-NH_2)—were obtained from the Keck Biotechnology Resource Laboratory (New Haven, CT). Using split synthesis, half of the peptide sample was modified at the N-terminus with 5,6-carboxy fluorescein (hereafter referred to as fluorescein) for use in fluorescence anisotropy experiments. Peptides were judged to be greater than 95% pure based on reversed-phase HPLC and MALDI-TOF conducted at the Univ. of Iowa.

2.3. Fluorescence anisotropy experiments

Fluorescence anisotropy experiments were conducted using a Fluorolog 3 (Jobin Yvon, Horiba) spectrofluorimeter. Fluorescence was monitored selectively using λ_{ex} of 496 nm, and λ_{em} of 520 nm with an 8 nm bandpass. Anisotropy (r) was calculated as shown in Eq. (1),

$$r = \frac{I_{VV} - G \cdot I_{VH}}{I_{VV} + G \cdot I_{VH}} \quad (1)$$

where I_{VV} and I_{VH} equal the intensities of vertically or horizontally emitted light upon vertical excitation, respectively, and G equals the instrument correction factor ($G = I_{HV} / I_{HH}$) where I_{HH} and I_{HV} equal the intensities of horizontally and vertically emitted light upon horizontal excitation, respectively. Averages of three readings with a 2 s. integration time at each point were recorded. The initial anisotropy was ~0.07 for Fl-hRyR1(3614–3643)p and ~0.05 for Fl-hRyR1(1975–1999)p. Samples containing 79 nM Fl-hRyR1(3614–3643)p or 200 nM Fl-hRyR1(1975–1999)p in

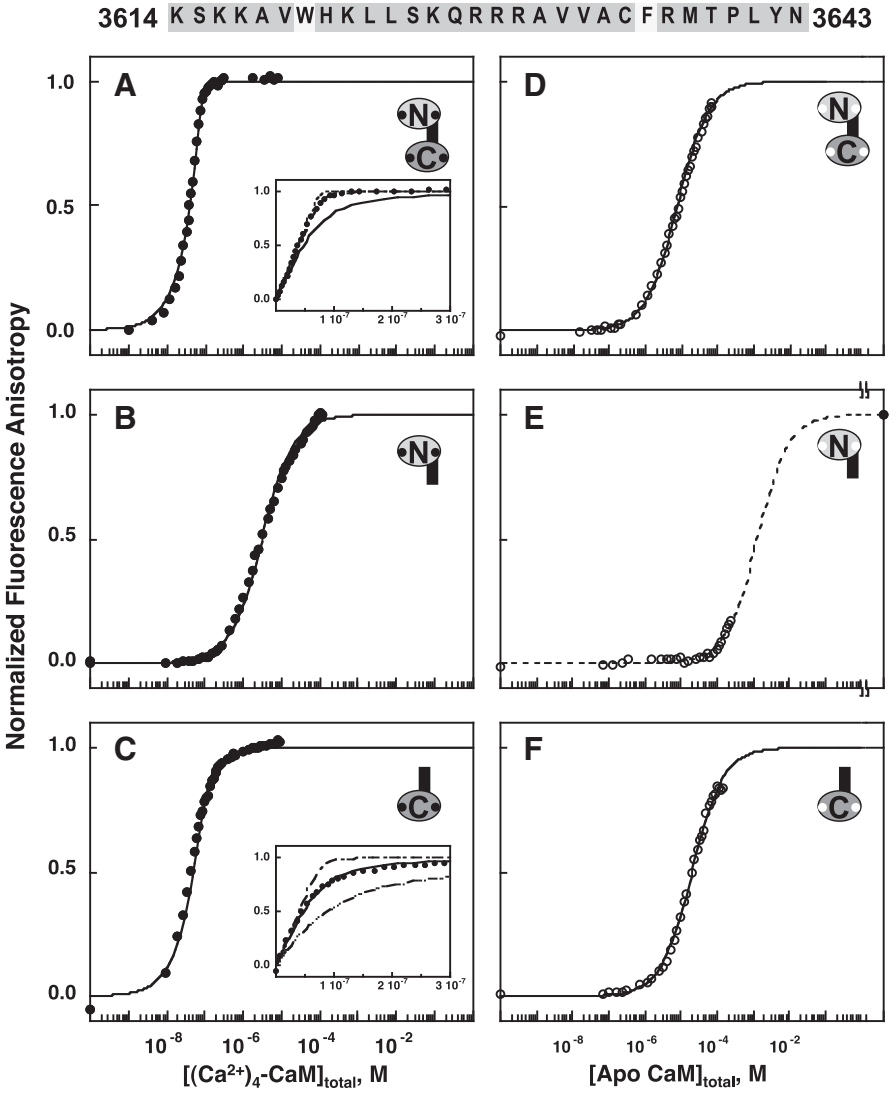

Fig. 2. Representative titrations of calcium-saturated (+10 mM $CaCl_2$; panels A–C) and apo (calcium-free; panels D–F) solutions of 79 nM Fl-hRyR1(3614–3643)p with CaM_{1-148}, CaM_{1-80}, and CaM_{76-148} as monitored by changes in fluorescence anisotropy. The amino acid sequence of hRyR1(3614–3643)p is depicted above the graphs. The solid curves depict simulations of fits to a one-site binding model (Eq. (3); Table 1A). Titration data for CaM_{1-148} and CaM_{76-148} are also depicted on a linear scale in the insets of panels A and C, along with simulated one-site K_d binding curves of 0.1 nM (- - -), 1 nM (– – – –), 10 nM (––––), and 50 nM (– – – –). The final anisotropy of the apo CaM_{1-80}:Fl-hRyR1(3614–3643)p solution (panel E) was estimated as the measured anisotropy after subsequent titration with concentrated calcium titrants (● symbol after break in the X-axis). This endpoint value was used as a fixed value for $Y_{[X]high}$ in estimating the K_d of the interaction between CaM_{1-80} and Fl-hRyR1(3614–3643)p by nonlinear least squares analysis.

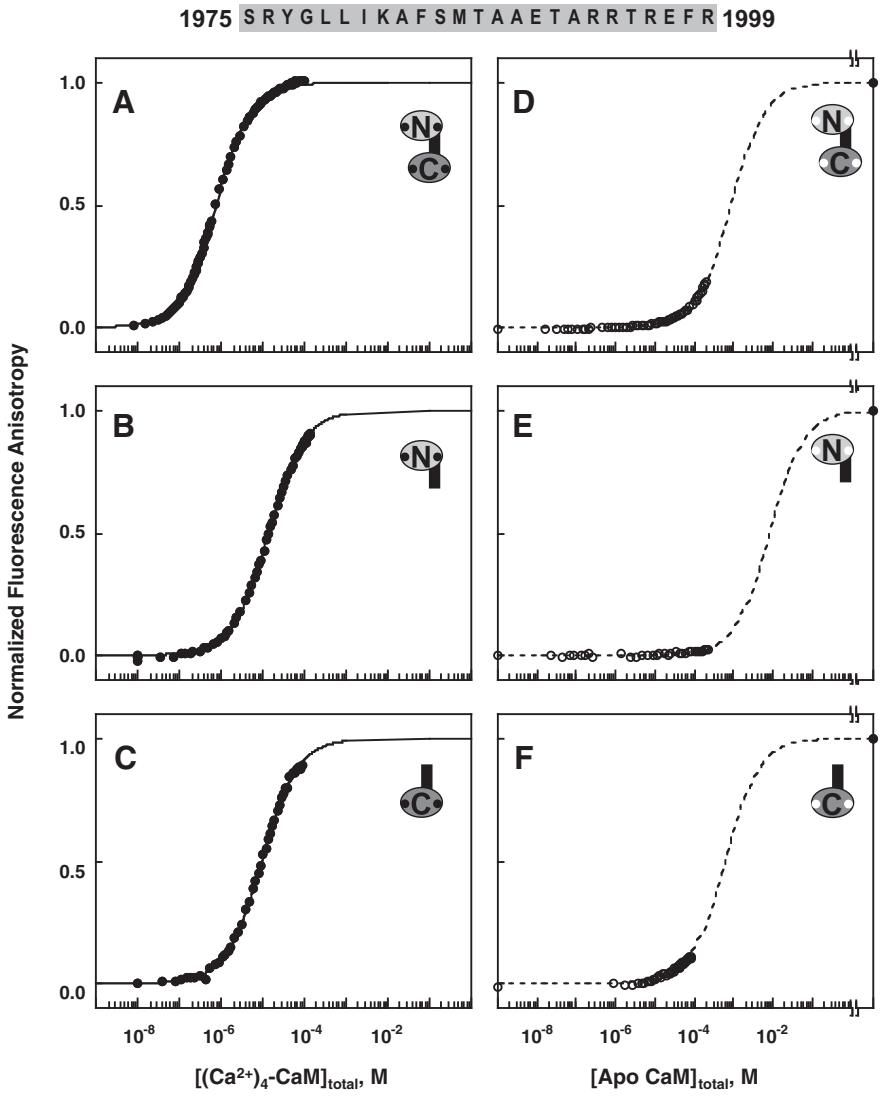

Fig. 3. Representative titrations of calcium-saturated (+10 mM $CaCl_2$; panels A–C) and apo (calcium-free; panels D–F) solutions of 200 nM Fl-hRyR1(1975–1999)p with CaM_{1-148}, CaM_{1-80}, and CaM_{76-148} as monitored by changes in fluorescence anisotropy. The amino acid sequence of hRyR1(1975–1999)p is depicted above the graphs. The final anisotropy values of the apo CaM:Fl-hRyR1(1975–1999)p solutions were estimated as the measured anisotropy after subsequent titration with concentrated calcium titrants (● symbol after break in X-axis in panels D–F). These values were used to fix $Y_{[X]high}$ in estimating the K_d of the interaction between CaM and Fl-hRyR1(1975–1999)p under apo conditions by nonlinear least squares analysis. Simulations of the fits to a one-site binding model (Eq. (3); Table 1B) are depicted by either solid (calcium-saturated) or dashed (apo) curves.

50 mM HEPES, 100 mM KCl, 50 μM EGTA, 5 mM NTA, 1 mM $MgCl_2$, pH 7.4 at 22 °C were titrated with concentrated solutions of CaM in the same buffer.

At least three titrations of each peptide were conducted under apo and calcium-saturating (i.e., in the presence of 10 mM $CaCl_2$) conditions. Representative sets of normalized data $((r - r_{min}) / (r_{max} - r_{min}))$ are shown in Figs. 2 and 3. For titrations in the absence of calcium, which did not approach saturation (see Figs. 2E and 3D–F), the anisotropy signal that would correspond to complete saturation of hRyR1 peptides was estimated by subsequently titrating the peptide–CaM solution with concentrated $CaCl_2$ solution in matching buffer, to a final calcium concentration of 5 mM. The addition of calcium is indicated in the figures by a break in the X-axis.

2.4. Determination of the dissociation constants for CaM binding to the hRyR1-derived peptides

Given that the peptide–CaM complex showed a 1:1 stoichiometry (data not shown), the affinity of apo and calcium-saturated CaM for the individual hRyR1 peptides was determined by fitting normalized titration data to a one-site Langmuir binding isotherm. Titrations of each peptide with CaM were analyzed by nonlinear least squares analysis using Eq. (2),

$$\overline{Y}_1 = \frac{K_a \cdot [X_{free}]}{1 + K_a \cdot [X_{free}]} \quad (2)$$

where $\overline{Y}_1$ is the fractional saturation of binding one CaM molecule to a peptide, K_a represents the association constant (the reciprocal of the dissociation constant, K_d) and $[X_{free}]$ equals the free concentration of CaM in solution. Approximating the free concentration of CaM by the total (i.e., $[X_{free}] \cong [X_{total}]$) is valid when the association is weak, and the dissociation constant is high relative to the peptide concentration. However, under stoichiometric conditions (i.e., where the K_d for CaM binding to the peptide was close to the concentration of peptide), the ligand (CaM) concentration is limiting. Therefore, in all titrations performed, the value of $[X_{free}]$ was estimated iteratively as the best solution to the difference between $[X_{total}]$ (calculated on the basis of the total ligand added) and $[X_{bound}]$, which was calculated as the product of the total peptide concentration ([peptide]) and $\overline{Y}_1$

Table 1
Affinity of Calmodulin for hRyR1 Peptides.

CaM	Apo		Calcium-saturated [a]		Fold change [b]
	K_d (μM)	ΔG[c] (kcal/mol)	K_d (μM)	ΔG[c] (kcal/mol)	
A. hRyR1(3614–3643)p					
$CaM_{1–148}$	6.79 ± 3.05	−7.02 ± 0.25	≤0.001	−12.15	~7000
$CaM_{1–80}$	~1500[d]	−3.81	2.50 ± 0.83	−7.59 ± 0.22	~600
$CaM_{76–148}$	24.89 ± 4.27	−6.22 ± 0.10	≤0.01	−10.80	~2500
B. hRyR1(1975–1999)p					
$CaM_{1–148}$	~850[d]	−4.14	0.66 ± 0.01	−8.34 ± 0.01	~1300
$CaM_{1–80}$	~7000[d]	−2.91	12.50 ± 1.95	−6.62 ± 0.09	~600
$CaM_{76–148}$	~650[d]	−4.30	9.21 ± 0.82	−6.80 ± 0.05	~70

[a] Standard buffer with 10 mM $CaCl_2$.
[b] Fold change = (K_d, Apo) / (K_d, Ca^{2+}).
[c] Free energy corresponding to estimated K_d; errors are reported only for cases where experimental errors could be determined for K_d.
[d] K_d estimated by fixing maximal anisotropy of titration as described in Materials and methods.

(the experimental observable). For high-affinity binding, the value of a dissociation constant estimated in this way correlates well with the precise numerical value of [peptide], which is subject to experimental inaccuracies. Thus, the dissociation constants for titrations performed under stoichiometric conditions are reported as limiting values in Table 1.

Experimental variations in the limits of the anisotropy signal of individual titrations of peptide were accounted for by Eq. (3),

$$f(X) = Y_{[X]low} + \overline{Y}_1 \cdot \left[\left(Y_{[X]high} - Y_{[X]low}\right) = Span\right] \quad (3)$$

where $Y_{[X]low}$ (low endpoint) corresponds to the fluorescence anisotropy of peptide alone, $\overline{Y}_1$ is the average fractional saturation of the peptide (Eq. (2)), and $Y_{[X]high}$ (high endpoint) corresponds to the anisotropy of the saturated peptide (*Span* represents the difference between the two endpoints). The formulation of Eq. (3) allows the value of either or both endpoint parameters to be set to a value(s) determined independently by experimentation (e.g., subsequent calcium titration of apo solutions to estimate the final anisotropies corresponding to complete saturation of RyR1 peptides in Figs. 2E and 3D–F) or test the dependence of resolved parameters on endpoint values. Three to six replicates of each titration were conducted. Representative sets of normalized data are shown in Figs. 2 and 3, and the results are summarized in a bar graph in Fig. 4.

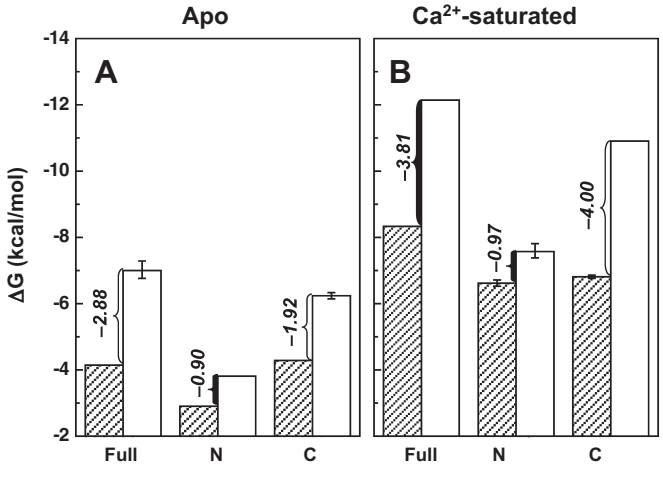

Fig. 4. Bar graph of free energies (ΔG; kcal/mol) associated with interactions between A. apo CaM and B. calcium-saturated CaM and either hRyR1(1975–1999)p (gray bars) or hRyR1(3614–3643)p (white bars); values and errors correspond to those presented in Table 1. The differences in free energy between CaM in the presence of the RyR1 peptides (ΔΔG = ΔG of CaM in the presence of hRyR1(3614–3643)p − ΔG of CaM in the presence of hRyR1(1975–1999)p) are also shown.

2.5. Equilibrium calcium titrations monitored by Phe and Tyr fluorescence

Fluorescence-monitored calcium titrations were conducted using SLM 4800™ (SLM Instruments Inc., Champaign-Urbana, IL) and PTI-QM4 (Photon Technology International, Birmingham, N.J.) fluorimeters. Calcium binding to sites I and II of the N-domain and to sites III and IV of the C-domain of CaM was studied in the absence and presence of hRyR1(1975–1999)p, as well as in the presence of hRyR1(3614–3643)p. In the case of hRyR1(1975–1999)p, domain-specific changes in the intensity of phenylalanine fluorescence were monitored with λ_{ex} of 250 and λ_{em} of 280 nm, and changes in the intensity of tyrosine fluorescence with λ_{ex} of 277 and λ_{em} of 320 nm, as described previously [5]. In the case of hRyR1(3614–3643)p, the same wavelengths were used for phenylalanine fluorescence intensity, but tyrosine was monitored at λ_{ex} of 270 nm and λ_{em} of 295 nm so that contributions from tryptophan in this peptide would be minimized, as described previously [35].

Each CaM sample (6 μM), either alone or with 2 equivalents of peptide (2 eq; 12 μM), was in a solution of 0.05–0.1 μM calcium indicator (Oregon Green 488 BAPTA-5N and/or X-Rhod-5F; Molecular Probes, Eugene, OR), 50 mM HEPES, 100 mM KCl, 50 μM EGTA, 5 mM NTA, 1 mM $MgCl_2$, pH 7.4, 22 °C and was titrated with a concentrated $CaCl_2$ solution containing the same buffer components. Note that the concentrations of buffer components listed are values for total solute concentration; the concentration of free Mg^{2+} varied as CaM was titrated with calcium. The concentration of free calcium at each titration point was determined by monitoring the fractional saturation of Oregon Green 488 BAPTA-5N (λ_{ex} of 494 nm, λ_{em} 521 nm; K_d for calcium of 34.24 μM) or X-Rhod-5F (λ_{ex} of 576 nm, λ_{em} of 603 nm; K_d for calcium of 1.78 μM) as described previously [36]. Three to six replicates of each titration were conducted. Representative sets of normalized data ($(F - F_{min}) / (F_{max} - F_{min})$) are shown in Fig. 5.

2.6. Analysis of free energies of calcium binding

Each CaM domain was analyzed as a 2-site binding system, as shown in the diagram below, where the intrinsic equilibrium constants are k_1 and k_2, and k_c represents any cooperativity between sites.

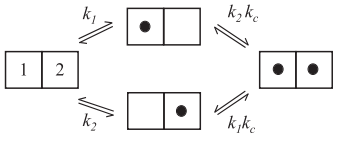

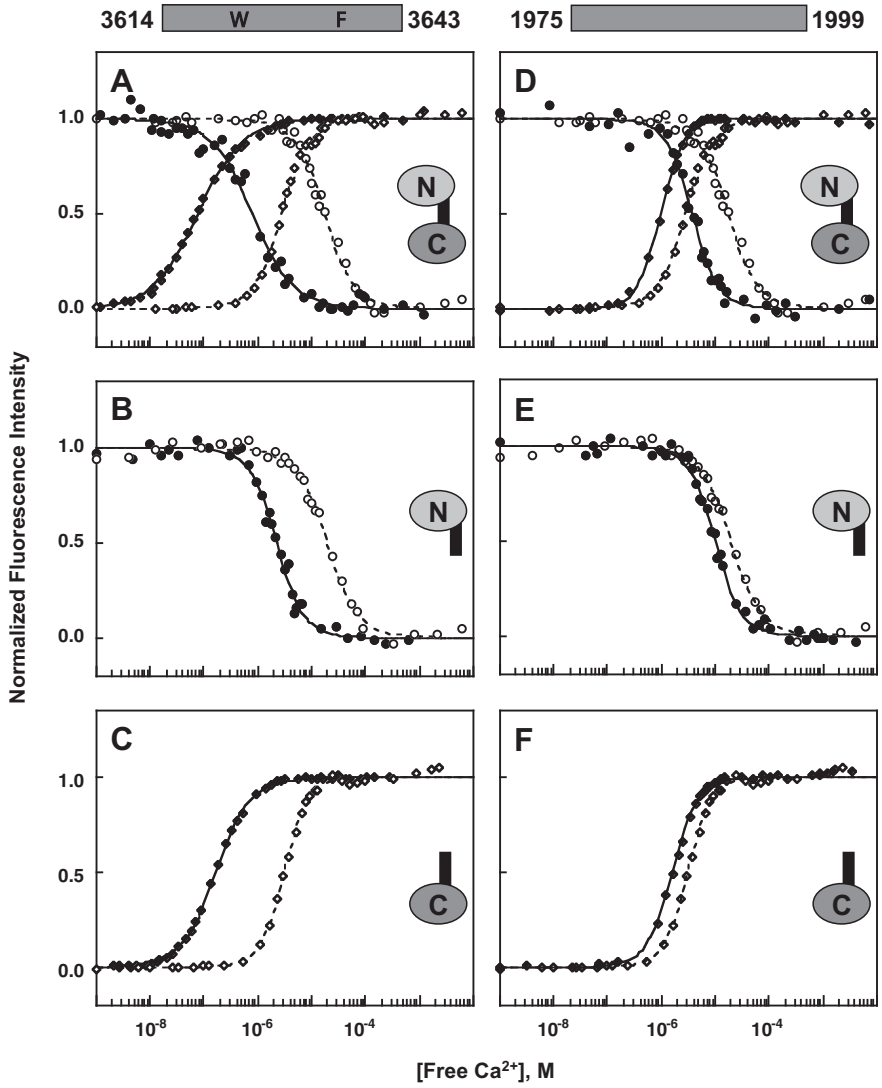

Fig. 5. Calcium titrations of 6 μM CaM_{1-148}, CaM_{1-80}, and CaM_{76-148} in the absence (open symbols) and presence (filled symbols) of 2 M equivalents of 12 μM hRyR1(3614–3643)p (panels A–C) or hRyR1(1975–1999)p (panels D–F) as monitored by changes in intensity of steady-state fluorescence of Phe (circles) or Tyr (diamonds). Lines through the data were simulated using the free energies resolved for calcium binding to CaM (Eq. (4); Table 2) in the absence (dashed curves) and presence (solid curve) of the hRyR1 peptide.

The Gibbs free energies of calcium binding to the CaM domains were determined by nonlinear least squares analysis, using a model-independent Adair function for saturation of two sites,

$$\overline{Y}_2 = \frac{K_1 \cdot [X] + 2 \cdot K_2 \cdot [X]}{2 \cdot (1 + K_1 \cdot [X] + K_2 \cdot [X]^2)} \quad (4)$$

where the macroscopic equilibrium constant K_1 is the sum of the two intrinsic equilibrium binding constants (k_1 and k_2), K_2 accounts for the total free energy of calcium binding to a domain (ΔG_2 is $-RT\ln(K_2)$) and is the product of k_1, k_2 and k_c, and [X] is the concentration of free calcium [37,38]. The formulation of Eq. (4) imposes no constraints on the relative values of k_1, k_2 and k_c; the sites may be non-equivalent and/or cooperative [37].

For nonlinear least squares analysis [39], the equilibrium calcium titrations were fit to a function [f(X)] that explicitly included terms to account for finite variations in the fluorescence signal at the asymptotes of the titrations, as described in Eq. (5),

$$f(X) = Y_{[X]low} + \overline{Y}_2 \cdot Span \quad (5)$$

where $Y_{[X]low}$ refers to the value of the fluorescence intensity in the absence of added calcium, $\overline{Y}_2$ (Eq. (4)) corresponds to the average fractional saturation of the two calcium-binding sites in each domain, and *Span* describes the magnitude of change in intensity (difference between high and low endpoints) and direction of change (i.e., positive for increasing fluorescence intensity and negative for decreasing fluorescence intensity) upon titration with calcium. These values were used to normalize the raw fluorescence intensity data for ease of comparison in Fig. 5.

In the absence of peptide, the free energies of calcium binding analyzed in this way represent the total free energy of binding. However, the apparent free energy of calcium binding is linked to the energy of peptide binding. In all cases studied, 2 eq of peptide did not fully saturate the apo CaM present at the beginning of each titration (i.e., under apo conditions). The initial concentration of CaM–peptide complex varied according to the affinities of apo CaM_{1-80}, CaM_{76-148} and CaM_{1-148} for each peptide. In calcium titrations of solutions containing hRyR1(3614–3643)p, the abundance of the apo complex was calculated to be ~64% for CaM_{1-148}, ~1% for CaM_{1-80}, and ~33% for CaM_{76-148}. In the presence of hRyR1(1975–1999)p, the abundance of each of those species was <2%. Therefore, values in Table 2 for calcium

Table 2
Effects of hRyR1 peptides on energies of calcium binding.

Protein	Peptide eq[a]	Peptide[b]	ΔG_1[c]	ΔG_2[c]	$\Delta\Delta G_2^{app}$[d]
A. Sites I and II (phenylalanine fluorescence)					
CaM_{1-148}	0		−6.17 ± 0.23	−12.76 ± 0.08	
	2	3614	−8.40 ± 0.03	−16.54 ± 0.18	−3.78 ± 0.20
	2	1975	−6.61 ± 0.50	−14.86 ± 0.28	−2.10 ± 0.29
CaM_{1-80}	0		−5.78 ± 0.29	−12.74 ± 0.02	
	2	3614	−6.93 ± 0.13	−15.36 ± 0.11	−2.62 ± 0.11
	2	1975	−6.25 ± 0.33	−13.56 ± 0.15	−0.82 ± 0.15
B. Sites III and IV (tyrosine fluorescence)					
CaM_{1-148}	0		−6.58 ± 0.24	−15.02 ± 0.02	
	2	3614	−10.00 ± 0.03	−18.85 ± 0.14	−3.83 ± 0.14
	2	1975	−6.81 ± 0.96	−16.11 ± 0.23	−1.09 ± 0.23
CaM_{76-148}	0		−6.15 ± 0.34	−14.85 ± 0.04	
	2	3614	−9.37 ± 0.31	−18.26 ± 0.13	−3.41 ± 0.14
	2	1975	−6.99 ± 0.56	−15.54 ± 0.08	−0.69 ± 0.09

[a] Molar ratios of CaM (6 μM) to peptide.
[b] 3614 refers to hRyR1(3614–3643)p, 1975 refers to hRyR1(1975–1999)p.
[c] Gibbs free energies (kcal/mol) determined from fits of 3 independent trials. Values from fits of CaM in the presence of peptide are reported as apparent Gibbs free energies (ΔG_n^{app} where n = 1 or 2) as described in Materials and methods.
[d] $\Delta\Delta G_2^{app} = \Delta G_2{}^{app}{}_{(CaM + peptide)} - \Delta G_{2(CaM\ alone)}$.

binding to CaM in the presence of 2 eq of peptide are reported as apparent Gibbs free energies (i.e., ΔG_1^{app} and ΔG_2^{app}).

3. Results

3.1. Affinity of CaM domains for hRyR1(3614–3643)p

Fluorescence anisotropy studies were conducted to determine the binding affinities of full-length CaM and its domains for Fl-hRyR1(3614–3643)p. Under conditions of saturating calcium, titrations of this peptide with CaM_{1-148} demonstrated that binding was in the stoichiometric range (i.e., 50% of the overall change in anisotropy, was achieved by the addition of 0.5 eq CaM_{1-148}; see Fig. 2A). To determine a limit for the dissociation constant, stoichiometric binding curves were simulated using multiple estimates of K_d (examples are shown in the inset of Fig. 2A); these indicated that the K_d was ≤1 nM.

Titrations of Fl-hRyR1(3614–3643)p with calcium-saturated domain fragments of CaM (CaM_{1-80} and CaM_{76-148}) are shown in Fig. 2. CaM_{1-80} (Fig. 2B) bound weakly, with a median ligand activity at ~100 eq, indicating that binding occurred under equilibrium conditions. Fractional saturation reached greater than 98% at ~100 μM total CaM_{1-80}, the highest concentration measured (Fig. 2B). Therefore, nonlinear least squares analysis (Eq. (3)) of titrations with CaM_{1-80} allowed simultaneous determinations of K_a, $Y_{[X]low}$, and $Y_{[X]high}$. The corresponding K_d was 2.50 ± 0.83 μM (Table 1A). In contrast, binding of calcium-saturated CaM_{76-148} (Fig. 2C) was judged to be stoichiometric, based on the observation that 50% of the change in anisotropy was complete after the addition of ~0.6 eq CaM_{76-148}. Based on a comparison to simulations such as those performed for CaM_{1-148}, the K_d was estimated to be ≤10 nM (inset of Fig. 2C). This was less favorable than the binding affinity of calcium-saturated CaM_{1-148} (by ~10-fold), but significantly more favorable (by 250-fold) than the binding affinity of the N-domain fragment.

Titrations of Fl-hRyR1(3614–3643)p with apo CaM_{1-148}, CaM_{1-80}, and CaM_{76-148} (Fig. 2D–F) demonstrated equilibrium (rather than stoichiometric) binding isotherms because the binding affinity was much lower than for calcium-saturated CaM. The titrations of peptide with apo CaM_{1-148} exceeded 90% saturation at the highest concentration of CaM measured (~60 μM) (Fig. 2D), and titrations with apo CaM_{76-148} exceeded 65% saturation (Fig. 2F). These values were fit to Eq. (3) using nonlinear least squares analysis, with simultaneous determination of K_a, $Y_{[X]low}$ and $Y_{[X]high}$. The K_d resolved for apo CaM_{1-148} was 6.79 ± 3.05 μM, while that for apo CaM_{76-148} was 24.89 ± 4.27 μM (i.e., a factor of 3.7 lower than that observed for CaM_{1-148}; Table 1A).

As illustrated in Fig. 2E, apo CaM_{1-80} had a much lower affinity for hRyR1(3614–3643)p than did either apo CaM_{1-148} or apo CaM_{76-148}. Even at ~200 μM total added CaM_{1-80}, less than 15% of the estimated overall change (i.e., determined by subsequent addition of calcium to the apo titration solution as described in the Materials and methods) in anisotropy for CaM-saturated Fl-hRyR1(3614–3643)p was complete. Therefore, in the nonlinear least squares analysis, it was necessary to set $Y_{[X]high}$ equal to that experimentally estimated endpoint, and to determine corresponding values for K_a and $Y_{[X]low}$. Titrations simulated based on these values are shown as dashed curves in Fig. 2E. The estimated K_d was ~1.5 mM, a factor of 220 times less favorable than that measured for apo CaM_{1-148} binding to this peptide. The actual dissociation constant may be even less favorable.

Comparison of binding to Fl-hRyR1(3614–3643)p under apo and calcium-saturating conditions indicated that calcium increased the affinity of CaM_{1-148} for the peptide by ~7000-fold, CaM_{1-80} by ~600-fold, and CaM_{76-148} by ~2500-fold (Table 1A).

3.2. Affinity of CaM domains for Fl-hRyR1(1975–1999)p

The relative affinities of CaM and its domains for hRyR1(1975–1999)p were determined in the same manner as those for Fl-hRyR1(3614–3643)p. All titrations of the peptide with calcium-saturated CaM_{1-148} (Fig. 3A), CaM_{1-80} (Fig. 3B), and CaM_{76-148} (Fig. 3C) reached greater than 85% saturation at concentrations of ~100 μM, and these titrations allowed simultaneous determination of K_a, $Y_{[X]low}$, and $Y_{[X]high}$. As shown in Table 1B, the estimated dissociation constant for calcium-saturated CaM_{1-148} (0.66 ± 0.01 μM) was more than an order of magnitude more favorable than those for CaM_{1-80} (12.50 ± 1.95 μM) and CaM_{76-148} (9.21 ± 0.82 μM).

In experiments performed in the absence of calcium, titrations of Fl-hRyR1(1975–1999)p with up to ~200 μM total CaM_{1-148} resulted in less than 20% of the predicted overall change in fluorescence anisotropy (see Fig. 3D). The upper limit of each titration ($Y_{[X]high}$) was estimated by adding calcium to the final titration solution, as described for the studies of CaM_{1-80} binding to Fl-hRyR1(3614–3643). Nonlinear least squares analysis was used to determine the most consistent values for K_a and $Y_{[X]low}$. The K_d for apo CaM_{1-148} binding was estimated to be at

least 850 μM (Table 1B). Titrations with CaM_{1-80} and CaM_{76-148} also indicated very weak associations. Less than 3% of the predicted change in anisotropy of the peptide was observed upon addition of ~200 μM CaM_{1-80} (Fig. 3E), and less than 11% of the predicted overall change was observed upon addition of ~80 μM CaM_{76-148} (Fig. 3F). Based on these titrations, limiting values of the weak dissociation constants were estimated as ~7 mM in the case of apo CaM_{1-80} and ~650 μM in the case of apo CaM_{76-148}. Titrations simulated with these values are shown as dashed curves in Fig. 3; the actual dissociation constants may be less favorable.

Comparing the binding of CaM to Fl-hRyR1(1975–1999)p under apo and calcium-saturating conditions, it was observed that calcium increased the affinity of CaM_{1-148} by ~1,300-fold, CaM_{1-80} by ~600-fold, and CaM_{76-148} by ~70-fold (Table 1B). As shown in Fig. 4, the domain-specific binding affinities of CaM for Fl-hRyR1(1975–1999) and Fl-hRyR1(3614–3643) were not equivalent under apo (Fig. 4A) or calcium-saturating conditions (Fig. 4B). In all pairwise comparisons, binding to Fl-hRyR1(3614–3643) (shown in white bars) was favored over binding to Fl-hRyR1(1975–1999)p (shown in gray bars). The corresponding values of the Gibbs free energies are given in Table 1.

3.3. Monitoring domain-specific calcium binding to CaM

Binding of calcium to sites III and IV in CaM_{1-148} causes a calcium-dependent increase in fluorescence intensity of residue Tyr138 located within site III (see Fig. 1A) in the absence [40,41] (open diamonds in Fig. 5A and D), and presence of hRyR1(3614–3643) (Fig. 5A; filled diamonds) or hRyR1(1975–1999) (Fig. 5D; filled diamonds). Binding of calcium to sites I and II causes a calcium-dependent decrease in the intrinsic steady-state fluorescence intensity of Phe residues in the absence of hRyR peptides (see open circles in Fig. 5A and D). Although the C-domain of CaM harbors three Phe residues, we previously established that for CaM alone (i.e., in the absence of exogenous peptide), domain-specific changes in calcium-dependent phenylalanine intensity reflect calcium binding to sites I and II in the CaM N-domain alone with no contribution from calcium binding to the C-domain [5]. However, in a study involving a peptide derived from the *Drosophila* RyR, we found that the CaM C-domain was disrupted such that it made a small contribution to the Phe signal [42].

To determine whether the binding of either hRyR1(3614–3643)p or hRyR1(1975–1999)p to CaM causes calcium-dependent changes in the Phe fluorescence intensity of the C-domain, we compared titrations of the peptides alone, and of CaM_{76-148} and CaM_{1-148} in the presence of 2 eq of each peptide. Calcium titrations of each RyR1 peptide alone showed no calcium-dependent changes in intrinsic Phe fluorescence intensity. There was a small change (<5%) in Phe intensity observed in the titration of CaM_{76-148} relative to the total signal change observed for CaM_{1-148} in the presence of each of these peptides (data not shown). Therefore, CaM association did not alter the contributions of Phe residues in the C-domain significantly, and the calcium-dependent changes in the Phe fluorescence of CaM-peptide complexes were interpreted to report exclusively on calcium binding to sites I and II.

3.4. hRyR1(3614–3643)p-induced changes in the calcium-binding properties of CaM

To explore the effect of hRyR1(3614–3643)p on the calcium-binding properties of the CaM domains (Fig. 5A–C), equilibrium calcium titrations of CaM alone (dashed curves, open symbols) were compared to those in the presence of hRyR1(3614–3643)p (solid curves, filled symbols). The total free energy (ΔG_2) of calcium binding to CaM_{1-148} alone was -12.76 ± 0.08 kcal/mol for sites I and II and -15.02 ± 0.02 kcal/mol for sites III and IV (see Table 2). These values reflect averages of determinations from 3 to 9 titrations. The solid curves through the data were simulated using best-fit parameters for the specific data set shown. As reported previously [3–5], a 10-fold difference in affinity of the two domains ($\Delta\Delta G_2$ of 2.26 kcal/mol) was observed.

In the presence of 2 eq of hRyR1(3614–3643)p (Fig. 5A, solid curves), the calcium-binding affinities of the N-domain (filled circles) and C-domain (filled diamonds) of CaM_{1-148} were increased significantly, as shown by the shift of the mid-point of the curves to lower calcium concentrations. Because 2 eq of hRyR1(3614–3643)p failed to fully saturate apo CaM_{1-148} present at the beginning of the titration (see Fig. 2D) the free energies of calcium binding to CaM_{1-148} in the presence of hRyR1(3614–3643)p are reported as apparent Gibbs free energies (ΔG_2^{app}, see Materials and methods). This was also observed in the studies of the domain fragments in the presence of hRyR1(3614–3643)p (see below) and the calcium titrations of CaM in the presence of hRyR1(1975–1999)p, and so values reported for those studies are also apparent Gibbs free energies.

The ΔG_2^{app} of calcium binding to CaM_{1-148} in the presence of hRyR1(3614–3643)p was -16.54 ± 0.18 kcal/mol for sites I and II and -18.85 ± 0.14 kcal/mol for sites III and IV, resulting in 3.78 ± 0.20 kcal/mol increase in affinity for sites I and II (see $\Delta\Delta G_2^{app}$ in Table 2A) and a 3.83 ± 0.14 kcal/mol increase in affinity for sites III and IV (see $\Delta\Delta G_2^{app}$ in Table 2B) relative to that observed in the absence of hRyR1(3614–3643)p.

The results for CaM_{1-148} were compared to those obtained for the CaM domain fragments (CaM_{1-80} and CaM_{76-148}). In the absence of hRyR1(3614–3643)p (dashed curve in Fig. 5B), the total free energy of calcium binding to CaM_{1-80} was -12.74 ± 0.02 kcal/mol and within the margin of error for the determination of calcium binding to sites I and II in the context of CaM_{1-148} (-12.76 ± 0.08 kcal/mol or $\Delta\Delta G_2$ of 0.02 ± 0.08 kcal/mol; Table 2A). However, the addition of 2 eq of hRyR1(3614–3643)p to CaM_{1-80} (solid curve in Fig. 5B) increased the apparent calcium-binding affinity of sites I and II to -15.36 ± 0.11 kcal/mol, which was 2.62 ± 0.11 kcal/mol more favorable than in the absence of hRyR1(3614–3643)p. This increase in affinity was not as great as the 3.78 ± 0.20 kcal/mol increase observed for the N-domain sites in CaM_{1-148} (Table 2A).

The total free energy of calcium binding to sites III and IV of CaM_{76-148} in the absence of peptide (dashed curve in Fig. 5C) was -14.85 ± 0.04 kcal/mol and slightly less favorable than that observed for CaM_{1-148} (-15.02 ± 0.02 kcal/mol or $\Delta\Delta G_2$ of 0.17 ± 0.04 kcal/mol; Table 2B). This small difference in binding affinity for sites III and IV in a fragment vs. in full-length CaM is consistent with previous observations [31]. The addition of 2 eq of hRyR1(3614–3643)p improved the apparent calcium-binding affinity of sites III and IV in CaM_{76-148} (solid curve in Fig. 5C) to -18.26 ± 0.13 kcal/mol, which was 3.41 ± 0.14 kcal/mol more favorable than in the absence of hRyR1(3614–3643)p (Table 2B). This was comparable to the peptide-induced difference observed for the same sites in CaM_{1-148} (3.83 ± 0.14 kcal/mol). A bar graph summarizing the energetics of calcium binding to CaM alone and in the presence of 2 eq hRyR1(3614–3643)p is shown in Fig. 6A–B.

3.5. hRyR1(1975–1999)p-induced change in the calcium-binding properties of CaM

Equilibrium calcium titrations of CaM_{1-148} conducted in the presence of 2 eq of hRyR1(1975–1999)p (solid curves in Fig. 5D) showed measurable increases in the calcium-binding affinities of sites within both domains when compared to CaM_{1-148} alone. The ΔG_2^{app} of calcium binding to sites I and II (closed circles) was -14.86 ± 0.28 kcal/mol (Table 2A), and 2.10 ± 0.29 kcal/mol more favorable than in the absence of hRyR1(1975–1999)p (open circles; see $\Delta\Delta G_2^{app}$ in Table 2A). The ΔG_2^{app} of calcium binding to sites III and IV (closed diamonds) of CaM_{1-148} was -16.11 ± 0.23 kcal/mol and $1.09 \pm$

0.23 kcal/mol more favorable than in the absence of hRyR1(1975–1999)p (open diamonds).

Equilibrium calcium titrations of CaM_{1-80} (Fig. 5E) and CaM_{76-148} (Fig. 5F) in the presence of hRyR1(1975–1999)p (solid curves) were compared to those in the absence of hRyR1(1975–1999)p (dashed curves) and to those for the same sites in CaM_{1-148}. The addition of 2 eq of hRyR1(1975–1999)p increased the apparent calcium-binding affinity of sites I and II of CaM_{1-80} (filled circles) to -13.56 ± 0.15 kcal/mol, which was 0.82 ± 0.15 kcal/mol more favorable than observed for CaM alone (open circles) and much smaller than the 2.10 ± 0.29 kcal/mol increase observed for CaM_{1-148} (see $\Delta\Delta G_2^{app}$ in Table 2A). Similarly, the addition of 2 eq of hRyR1(1975–1999)p increased the apparent calcium-binding affinity of sites III and IV in CaM_{76-148} (filled diamonds) to -15.54 ± 0.08 kcal/mol which was 0.69 ± 0.09 kcal/mol more favorable than that observed for CaM alone (open diamonds) and much smaller than the 3.41 ± 0.14 kcal/mol increase caused by hRyR1(3614–3643) (Table 2B). A set of bar graphs summarizing the domain-specific energetics of calcium binding in the absence and presence of hRyR1(1975–1999)p is shown in Fig. 6C and D.

It must also be noted that given the very weak association between apo CaM and hRyR1(1975–1999)p, the level of saturation of apo CaM at 2 eq of hRyR1(1975–1999)p was not complete at the start of the calcium titrations of CaM_{1-148}, CaM_{1-80} and CaM_{76-148}; obtaining complete saturation would not be experimentally feasible. In acknowledgment of this limitation, we have been careful to report resolved values of free energies as apparent values. Likewise, we must also be careful in our comparisons of the $\Delta\Delta G_2^{app}$ values calculated for CaM in the presence of hRyR1(1975–1999)p, and recognize that these differences may underestimate the actual differences since these data clearly show association with hRyR1(1975–1999)p increases the calcium affinity of CaM.

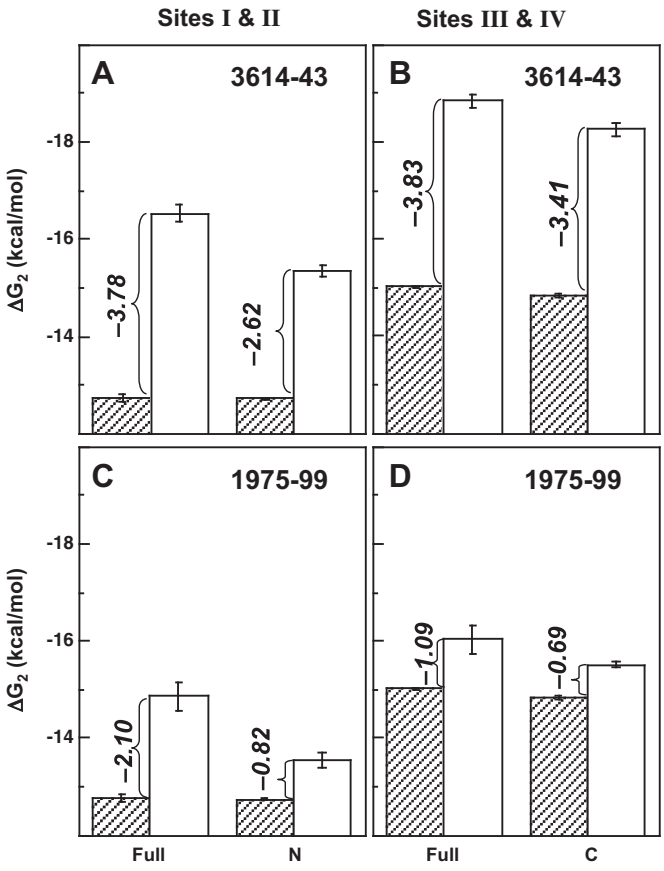

Fig. 6. Effect of hRyR1(3614–3643)p and hRyR1(1975–1999)p on the energetics of calcium binding to CaM. Bar graph of apparent total Gibbs free energies of calcium binding to CaM (ΔG_2^{app}; kcal/mol) in the absence (gray bar) and presence (white bar) of hRyR1(3614–3643)p (panels A and B) or hRyR1(1975–1999)p (panels C and D). These results are based upon equilibrium titrations shown in Fig. 5, and reflect the values in Table 2. The change in apparent free energy upon binding of the hRyR1 peptide ($\Delta\Delta G_2^{app} = \Delta G_2^{app}$ of CaM in the presence of hRyR1p $- \Delta G_2^{app}$ of CaM alone) is also highlighted.

4. Discussion

Physiological and biochemical studies have shown that the two CaM domains have separable roles in regulating the homo-tetrameric RyR1, and that they interact with multiple CaM-binding regions on RyR1 [16,26,27,43]. The studies presented here explore the molecular basis of CaM-mediated regulation of RyR1 by measuring the energetics of association of full-length CaM and its individual domains with sequences representing two of these regulatory regions of human RyR1: hRyR1(1975–1999)p and hRyR1(3614–3643)p.

4.1. Domain-specific binding of CaM to hRyR1(3614–3643)p

Titrations monitored by fluorescence anisotropy (Fig. 2) indicate that CaM_{1-148} binds to hRyR1(3614–3643)p with very high affinity (sub-nanomolar K_d) at high calcium concentrations, and with significantly weaker affinity (low micromolar K_d) in the absence of calcium (Table 1). Titrations with the domain fragments of CaM (Fig. 2) show that the C-domain of CaM interacts with the 3614–3643 region in a calcium-independent manner, while the N-domain requires calcium for association. Both in the presence and in the absence of calcium, the C-domain serves as the dominant mediator of association between CaM and hRyR1(3614–3643)p: the C-domain fragment has an affinity for 3614–3643 that is 2 orders of magnitude more favorable than the N-domain fragment. This difference is consistent with previous qualitative studies of CaM-induced changes in the emission spectra of Trp3620 of non-fluoresceinated hRyR1(3614–3643)p [26]. Several other CaM-binding targets are known to preferentially bind to the C-domain of apo CaM_{1-148} with subsequent calcium-dependent association of the N-domain; examples include NMDA receptor NR1 subunit [44], voltage-dependent sodium channel $Na_V1.2$ [45], and calcium-dependent small conductance K^+ (SK) channels [14]. Despite this commonality, the mechanism of CaM-mediated regulation of ion channels also depends on the relative affinity of the channel for apo vs. calcium-saturated CaM and the stoichiometry of CaM binding. For instance, $Na_V1.2$ has a higher affinity for apo CaM than for calcium-saturated CaM, while hRyR1(3614–3643)p has a higher affinity for calcium-saturated CaM than for apo CaM.

The affinity of apo CaM for the 3614–3643 region of RyR1 is much weaker than previously reported by Hamilton and coworkers from binding studies using the intrinsic fluorescence of the single tryptophan in hRyR1(3614–3643)p [16], but is consistent with the results of a very recent ITC study of the interaction between CaM and several regulatory regions of RyR1 and RyR2 isoforms [46]. Importantly, this affinity is much less favorable than that for the full-length receptor (low micromolar compared to low nanomolar), indicating that residues outside the 3614–3643 sequence contribute to the interaction with apo CaM.

A difference between our study and the ITC experiments by the Van Petegem laboratory [46] involves the relative contributions of each domain of apo CaM to the interaction. While the ITC study suggested that the N-domain primarily contributes to binding to hRyR1(3614–3643)p (K_d of 46.5 μM for full-length CaM and 55.6 μM for the N-domain fragment), our estimates indicate that binding of CaM was dominated by the contribution of the C-domain (CaM_{76-148}) in the absence of calcium. There are slight differences in the solution conditions and boundaries of the CaM domains used in these studies. It would be surprising, but interesting, if these alone accounted for such a large difference.

The studies agree that the interaction in the presence of calcium is very strong and that the C-domain binds much more favorably than the N-domain. However, our study found significantly tighter binding of full-length CaM and each of the domains to hRyR1(3614–3643). For example, our K_d estimate for CaM_{1-148} is ≤1 nM, much lower than the value (46 nM) estimated by ITC [46]. A similar difference is seen for the K_d values reported for individual CaM domains. This may be explained by signal detection differences in the methods. ITC must use higher concentrations of peptide and CaM than were used in the titrations monitored by fluorescence anisotropy, making it more challenging to estimate a very low (high affinity) equilibrium dissociation constant.

4.2. Domain-specific binding of CaM to hRyR1(1975–1999)p

Although both domains of calcium-saturated CaM can associate with the 3614–3643 site on each RyR1 monomer, it has been hypothesized that the N-domain preferentially associates with the 1975–1999 region on a neighboring RyR1 subunit [27]. Such an interaction would be analogous to the association of calcium-saturated CaM with the 1.3 MDa γ-subunit of phosphorylase kinase, in which the calcium-saturated domains of CaM simultaneously interact with two non-contiguous CaM-binding motifs (i.e., Ph5 and Ph13) at very high affinity and in an elongated conformation [47–49]. An extended conformation of CaM is also seen in the complexes with the SK channel calmodulin-binding domain, in which the N- and C-domains of CaM bridge between two channel monomers, and the Anthrax Edema Factor (Fig. 1E, F) [13,14]. It was postulated that the intrinsic sequence of the 1975–1999 site would be sufficient to mediate a strong association with the N-domain of CaM.

However, in contrast to studies of the 3614–3643 CaM-binding domain, titrations of Fl-hRyR1(1975–1999)p demonstrated negligible binding of CaM_{1-148} or either CaM domain in the absence of calcium. At high calcium concentrations, the sub-micromolar affinity (K_d of 660 nM; Table 1) observed for CaM_{1-148} was shown to result from relatively weak contributions from both domains (~10 μM for CaM_{1-80} and CaM_{76-148}). Such higher-affinity binding via covalent linkage of CaM domains has also been shown for CaM binding to a peptide derived from CaMKII [50]. Interestingly, CaMKII and hRyR1(1975–1999)p lack a bulky hydrophobic anchor residue (such as Trp) adjacent to a positively charged cluster (Fig. 1C), which is typically found in targets that utilize the C-domain as the predominant mediator of the interaction, as in the case of hRyR1(3614–3643)p (shown here; Fig. 1D) and several other targets including NR1C0p of the NMDA receptor [44], skMLCK [51], and melittin [35].

The observed interaction between calcium-saturated CaM_{1-148} and hRyR1(1975–1999)p is consistent with findings from previous studies [27,46]. In particular, our estimates of the dissociation constants of calcium-saturated CaM_{1-148}, CaM_{1-80} and CaM_{76-148} binding to hRyR1(1975–1999)p agree very closely with the values obtained by Van Petegem and colleagues from ITC experiments [46]. Our failure to observe a calcium-independent association of CaM_{1-148} with hRyR1(1975–1999)p, as previously reported by Zhang et al., [27] may be attributed to the inclusion of 1 mM $MgCl_2$ in our experiments which had been expected to help mimic physiological intracellular conditions. Magnesium has previously been shown to associate with CaM and to significantly decrease the affinity of calcium-free and calcium-saturated CaM–target interactions [52–54]. However, the ITC studies, also performed in the absence of magnesium, have also failed to detect an interaction between apo calmodulin and this site [46]. The weak binding may also reflect a limitation of using a peptide as a model of the binding site as it appears within the tertiary structure of the complete RyR1 subunit. While this study and the ITC results agree that the binding of full-length apo CaM and its domains to this site is very weak, we were able to report for the first time estimates of limiting values for the dissociation constants of interaction (Table 1).

4.3. Effects of hRyR1(3614–3643)p and hRyR1(1975–1999)p on calcium binding

Many CaM-binding motifs induce significant changes in the calcium-binding properties of CaM, serving as allosteric effectors that allow CaM to regulate individual target proteins at different levels of intracellular calcium. Peptide association can lead to either an increase [55–57] or a decrease [45,58] in the affinity of CaM for calcium, and can even affect the two CaM domains differentially [35,36,59,60]. The allosteric effect of hRyR1(3614–3643)p on the calcium affinity of each CaM domain was dramatic and identical within the margin of error (i.e., $\Delta\Delta G_2^{app}$ of -3.78 ± 0.18 kcal/mol for sites I and II and $\Delta\Delta G_2^{app}$ of -3.83 ± 0.14 kcal/mol for sites III and IV), indicating that the ten-fold difference in the intrinsic calcium-binding affinities of sites in the N- and C-domains was maintained when CaM associated with hRyR1(3614–3643)p (Table 2). The midpoints of titrations of calcium binding to the N- and C-domains of CaM in the presence of the peptide were ~1 μM and ~100 nM, respectively (Fig. 5A). Similar RyR1(3614–3643)p-induced increases in the calcium binding affinities of the two CaM domains were observed in a previous study that used a full-length CaM in which a pyrene moiety was introduced at T34C (within the N-domain), or at T110C (within the C-domain) [28]. In contrast, calcium-binding studies with engineered calmodulins containing tryptophan residues in either the N-or C-domain (F19W and F92W, respectively) reported an effect of RyR1(3614–3643)p binding on the calcium affinity of the C-, but not the N-domain of CaM [26]. The maintenance of the ten-fold difference in the calcium-binding affinities of the CaM N- and C-domains observed in these studies is similar to that observed for CaM bound to a calcineurin sequence [61], but in stark contrast to the effects of the CaM-binding sequences from CaMKII [36], MLCK, CaATPase [60] and the bee venom peptide melittin [35], which equalize the calcium-binding affinities of the CaM N- and C-domains.

Equilibrium calcium titrations of CaM_{1-148} in the presence of hRyR1(1975–1999)p also showed significant increases in the calcium-binding affinities of both domains ($\Delta\Delta G_2^{app}$ of -2.10 ± 0.29 kcal/mol for sites I and II and -1.09 ± 0.23 kcal/mol for sites III and IV). However, in contrast to results from titrations in the presence of hRyR1(3614–3643)p, hRyR1(1975–1999)p induced a 1.01 ± 0.37 kcal/mol greater increase in the calcium-binding affinities of the N-domain sites relative to those of the C-domain (Table 2). These domain-specific changes reduced the ~10-fold difference in intrinsic calcium-binding affinities of the CaM domains to ~3-fold in the presence of hRyR1(1975–1999)p, allowing for overlap in the titrations of the two domains, as previously observed for CaM in the presence of melittin [42] and nitric oxide synthase [62].

In addition to peptide-induced effects on the intrinsic calcium-binding properties of the pair of sites in each CaM domain, interdomain cooperativity has been observed in the presence of skMLCK, mastoporan, and cerebellar nitric oxide synthase [62,63]. Comparing the effect of hRyR1(3614–3643)p on calcium binding to sites I and II in CaM_{1-80} and CaM_{1-148} indicated that the presence of the C-domain made the calcium-binding free energy (ΔG_{app}) more favorable by 1.16 ± 0.25 kcal/mol. In contrast, the values of $\Delta\Delta G_2^{app}$ for sites III and IV in CaM_{76-148} and CaM_{1-148} were indistinguishable within the reported standard deviation reported in Table 2, indicating that, in the presence of hRyR1(3614–3643)p, the N-domain had no significant effect on the calcium-binding affinity of the C-domain in CaM_{1-148}.

Equilibrium calcium titrations of CaM_{1-80} and CaM_{76-148} in the presence of hRyR1(1975–1999)p also demonstrated increases in the calcium-binding affinities of sites within both CaM fragments. However, as observed for titrations of CaM_{1-80} in the presence of hRyR1(3614–3643)p, the addition of hRyR1(1975–1999)p resulted in a smaller increase in the calcium-binding affinity of sites I and II of CaM_{1-80} ($\Delta\Delta G_2^{app}$ of −0.82 kcal/mol) than in sites I and II of CaM_{1-148} ($\Delta\Delta G_2^{app}$ of −2.10 kcal/mol), indicating that the C-domain affects the

properties of the N-domain within CaM_{1-148}. In contrast, the values of $\Delta\Delta G_2^{app}$ for sites III and IV of CaM_{76-148} (-0.69 ± 0.09 kcal/mol) and CaM_{1-148} (-1.09 ± 0.23 kcal/mol) were each within the margins of error for the other, indicating that the N-domain had no significant effect on the calcium-binding affinity of the CaM C-domain. Taken together, the calcium binding titrations in the presence of the two RyR1 peptides show a small degree of interdomain cooperativity for the weaker N-domain, but not the stronger C-domain calcium-binding sites. This is consistent with the results of a theoretical analysis of the distribution of the free energy of cooperativity between non-identical sites in a two-site macromolecule [35,64]. The interdomain cooperativity observed in the presence of hRyR1(3614–3643)p indicates that the two domains of CaM do not function independently (i.e. there are energetic interactions), similarly to what has been observed in many other CaM–target interactions, even though in the complex with the (3614–3643) peptide the structural coupling between the CaM domains is weak [19,20].

4.4. Models of the calcium dependence of domain-specific interactions of CaM with RyR1

Based on comparison of the energetics of CaM association with hRyR1(1975–1999)p and hRyR1(3614–3643)p, two models of domain-specific association in the context of the RyR1 tetramer are proposed (Fig. 7). Comparison of the relative affinities of the domains of apo CaM for hRyR1(1975–1999)p versus hRyR1(3614–3643)p shows that the C-domain binds weakly to the 3614–3643, but not to the 1975–1999 region, while the N-domain does not interact measurably with either site. This suggests that a complex of apo CaM with RyR1 exists in which CaM is tethered to RyR1 by association of its C-domain with the 3614–3643 CaM-binding motif as depicted in Fig. 7A. Alternatively, the N-domain of apo CaM simultaneously binds to a still unidentified region on the channel. Given the significantly higher affinity of apo CaM for the full-length channel [16] compared to the 3614–3643 sequence, it is likely that there are additional binding site(s) for apo CaM on the receptor. Residues in the vicinity of the 3614–3643 region might contribute to the interaction, increasing the binding affinity. Based on the low micromolar affinity of calcium-free CaM for region (4295–4325) of hRyR1, Van Petegem and colleagues have proposed that this region represents a binding site for apo CaM [46]. Cryo-EM studies have shown that, in the absence of calcium, CaM binds to a site on the receptor located in domain 3 close to domain 4 [17,25], but the exact sequence of this region is unknown. Additional sequence mapping studies will be needed in order to identify all RyR1 residues involved in the association with apo CaM.

Under calcium-saturating conditions, comparison of relative affinities of the domains of CaM for the two CaM-binding motifs suggests that the C-domain of CaM remains bound preferentially to the 3614–3643 CaM-binding motif ($\Delta\Delta G \leq -4.00$ kcal/mol). However, under physiological concentrations of CaM (i.e., 2–25 μM [65–67]), the calcium-saturated N-domain of CaM can associate with either the 3614–3643 (Fig. 7B) or 1975–1999 (Fig. 7C) regions. However, the affinity of the N-domain of CaM for hRyR1(3614–3643)p was shown to be approximately 5-fold higher ($\Delta\Delta G$ of -0.97 ± 0.24 kcal/mol) than that for hRyR1(1975–1999)p. This preference of N-domain association with hRyR1(3614–3643)p was further confirmed by the fact that fluorescence-monitored calcium titrations in the presence of both CaM-binding domains were identical to those seen for CaM in the presence of 3614–3643 alone (data not shown). These data indicate that the intrinsic properties of the CaM-binding sequences in the context of the full-length receptor support intra-subunit binding of the N-domain as shown in Fig. 7B. Nonetheless, conformational rearrangements in the full-length receptor could occlude the CaM N-domain binding site of hRyR1(3614–3643)p, allowing CaM to bridge the two CaM-binding regions (Fig. 7C). While FRET studies using fluorophore-labeled CaM and FKB12.6 in the context of full-length RyR1 suggest similar locations for apo and Ca^{2+}–CaM on the channel [68], cryo-EM data support Ca^{2+}–CaM binding at the gap between domains 3 and 7, at a distinct but partially overlapping location compared to apo CaM [17]. As in the case of apo CaM, additional studies will be needed in order to identify the exact RyR1 sequences corresponding to these locations.

Based upon the models presented in Fig. 7 and the free energies of calcium binding to CaM_{1-148} in the presence of the individual CaM-binding motifs (Table 2), the fractional saturation of the domains of CaM_{1-148} in the context of the homo-tetrameric RyR1 can be predicted. If both domains of CaM_{1-148} associate with the 3614–3643 region of RyR1, then the calcium-binding affinities of the N- and C-domain sites would be separated by approximately 10-fold, as illustrated in Fig. 7B. However, if the N-domain of CaM preferentially associates with the 1975–1999 region of RyR1, while the C-domain of CaM remains associated with the 3614–3643 region, then the calcium-binding affinity of the N- and C-domain sites of CaM_{1-148} would be separated by approximately 30-fold, as illustrated in Fig. 7C.

Given the variation in stability and solubility of CaM target proteins, synthetic peptides representing their CaM-binding motifs are often used to model target association with CaM. In most instances CaM interaction with the peptide correlates well with properties of CaM binding in the context of the full-length target. For example, as observed by HSQC NMR, the backbone structures of ^{15}N–CaM bound to a peptide representing the CaM-binding motif of CaMKI and ^{15}N–CaM bound to the full enzyme were shown to be virtually identical [69]. Furthermore, many of the properties of CaM interacting with hRyR1(3614–3643)p have been shown to correlate well with properties of CaM binding in the context of the full channel [28]. However, there are instances that have demonstrated increased [70] or decreased [71] affinity of CaM for a peptide relative to the full-length target; presumably these reflect the absence of tertiary constraints of the full-length target that may be favorable or unfavorable to CaM binding.

Previous studies have reported that CaM switches from an activator to an inhibitor of RyR1 at concentrations of calcium greater than 1 μM [18,43,72], and it has been hypothesized that the distinct functional roles of CaM in regulating channel activity are due to calcium binding to each domain of CaM. The models presented here are consistent with those proposed for the C-domain association to RyR1, whereby the C-domain of CaM binds constitutively to the 3614–3643 region of RyR1, acting as an anchor for the channel at all calcium concentrations [26,28]. However, conflicting evidence for N-domain binding to RyR1 has led to multiple models for its role in the regulation of the receptor. CaM site-knockout mutations (E31Q/E67Q [73] or E31A/E67A [43]) that abolish calcium binding to the N-domain do not have a significant effect on CaM regulation of channel closure, suggesting that calcium binding to the N-domain of CaM is not essential for the ability of CaM to inhibit RyR1 activity. Instead, it was proposed that calcium binding to the C-domain switches CaM from an activator to an inhibitor of RyR1 [73]. On the other hand, Bigelow and colleagues have proposed that calcium binding to the N-domain of CaM at micromolar cytoplasmic Ca^{2+} levels triggers conformational changes in both CaM domains that lead to closing of the channel. The importance of the N-domain in channel regulation is also demonstrated by the fact that deletions or extensions at the N-terminus of CaM cause a significant increase or decrease, respectively, in the ability of CaM to inhibit RyR1 [26].

Studies investigating the location of the two CaM domains on RyR1 have proposed that the C-domain stays bound to the 3614–3643 region at all calcium concentration, while the N-domain binds to this site only at high Ca^{2+} and then with lower affinity than the C-domain [26]. It has also been proposed that the N-domain of CaM interacts with the 1975–1999 sequence of RyR1, such that CaM regulates the activity of the channel by acting at a site of inter-subunit contact that modulates the opening and closing of the transmembrane pore [27]. Our results presented here indicate that binding of the N-domain to either the (3614–3643) or (1975–1999) region is calcium-linked, and that the

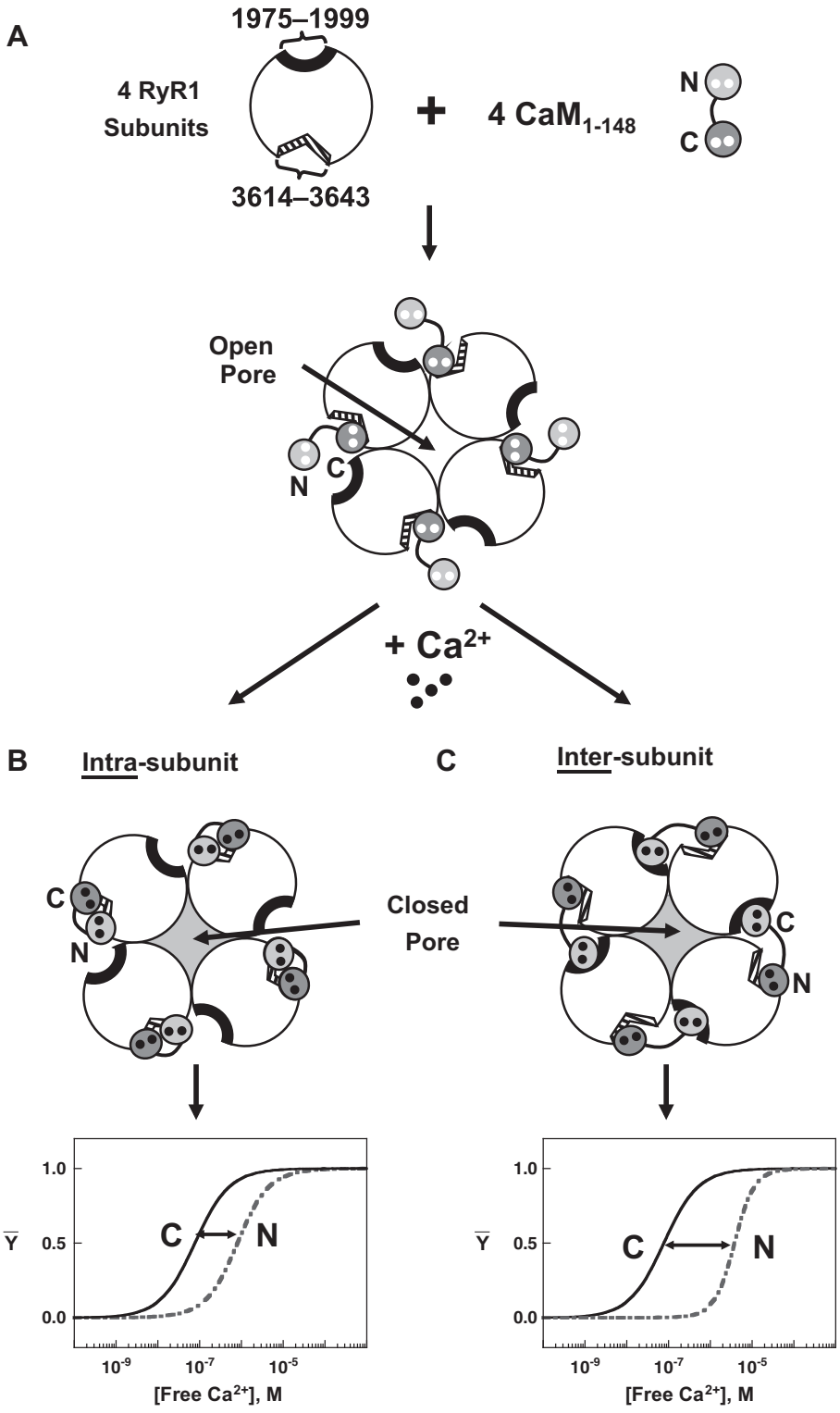

Fig. 7. Models of CaM interaction in the context of the RyR1 homotetramer. These cartoons depict the view from the cytoplasmic face of the RyR1 tetramer, with each RyR1 subunit represented as a white sphere. The 3614–3643 CaM-binding motif is represented as a hatched triangular surface, whereas the 1975–1999 CaM-binding motif is represented by a black concave surface. The CaM N- and C-domains are highlighted and connected by the flexible linker region of CaM (black line). A. Under apo conditions, CaM is bound to RyR1 subunits via its C-domain, through interactions with the 3614–3643 CaM-binding motif. Upon calcium ligation, the C-domain undergoes a calcium-induced change in binding position on the 3614–3643 CaM-binding motif. In B. the "Intra-subunit" Model, the calcium-saturated N-domain associates with the 3614–3643 CaM-binding motif, whereas in C., the "Inter-subunit" Model, the calcium-saturated N-domain associates with the 1975–1999 CaM-binding motif of an adjacent subunit. Simulations based upon the calcium-binding affinities of the CaM_{1-148} domains in the presence the individual CaM-binding motifs (Table 2) are shown for the fractional saturation of the CaM_{1-148} N-domain (dashed gray line) in the presence of hRyR1(3614–3643)p (panel B) or hRyR1(1975–1999)p (panel C), together with the fractional saturation of the C-domain sites (solid black line) in the presence of hRyR1(3614–3643)p (panels B and C).

affinity for the N-domain of calcium-saturated CaM is higher for hRyR1(3614–3643)p than for hRyR1(1975–1999)p. Therefore, for the calcium-loaded N-domain to favor binding to 1975–1999 over 3614–3643 in the context of homo-tetrameric RyR1 there must be additional tertiary constraints. For example, a previous study demonstrated that region 4064–4210 of RyR1 is structurally and functionally similar to a domain fragment of CaM and therefore may provide an additional level of allosteric control by competing with CaM domains for binding to the 3614–3643 CaM-binding domain [74]. In addition, residues that are spatially proximal to the 1975–1999 CaM-binding motif in the folded structure of RyR1 could contribute to an overall binding interface that is more favorable energetically than what the peptide alone offers. If indeed the C-domain of CaM is constitutively bound to the (3614–3643) region in the context of full-length RyR1, our calcium-binding titrations suggest that this domain is calcium-loaded in the resting muscle, and its movement between different sites within this region may play a role in channel activation. According to the simulations shown in Fig. 7, the N-domain is predicted to play a role in inhibition of RyR1, especially in the presence of hRyR1(1975–1999)p where the N-domain sites only begin to saturate at concentrations of calcium greater than 1 μM.

5. Summary

The studies presented here comprise a thermodynamic analysis of how two RyR1 sequences, 1975–1999 and 3614–3643, interact with CaM, an allosteric effector of receptor function. The differences in domain-specific interactions support a model of RyR1 regulation in which CaM activates RyR1 via association of the apo C-domain with the 3614–3643 CaM-binding motif under the low calcium conditions of a resting muscle, poising the N-domain of CaM to inhibit RyR1 function via calcium-dependent association with a distinct site. This provides a clear example of how the domains of CaM have separable roles in regulating RyR1 and the advantages of having more than one CaM-binding sequence in each subunit of a multimeric target protein. RyR1 is one of many channels now recognized to use CaM to modulate calcium-triggered conformational change linked to the regulation of its quaternary structure. It will be interesting to see whether the division of labor or chemical work observed in this case will apply more generally as the energetics and linkage inherent in those systems (e.g., the NMDA receptor, and voltage-gated calcium and sodium channels) are explored in greater detail.

Acknowledgments

We thank Lynn Teesch and Elena Rus for amino acid analysis (Univ. of Iowa, Molecular Analysis Facility); Shapoor Riahi for atomic absorption analysis (Univ. of Iowa, Dept. of Pediatrics); Chris Blaumueller (Univ. of Iowa, Dept. of Anatomy and Cell Biology); Susan O'Donnell and T. Idil Apak Evans for critical reading of the manuscript. This study was supported by a University of Iowa Center for Biocatalysis and Bioprocessing NIH Biotechnology Training grant (NIH T32 GM08365) to R.A.N., a University of Iowa Carver College of Medicine FUTURE in Biomedicine Fellowship to A.M.K. and a grant from the National Institutes of Health (R01 GM 57001) to M.A.S.

References

[1] K.P. Hoeflich, M. Ikura, Calmodulin in action: diversity in target recognition and activation mechanisms, Cell 108 (2002) 739–742.
[2] G. Barbato, M. Ikura, L.E. Kay, R.W. Pastor, A. Bax, Backbone dynamics of calmodulin studied by ^{15}N relaxation using inverse detected two-dimensional NMR spectroscopy: the central helix is flexible, Biochemistry 31 (1992) 5269–5278.
[3] M. Ikura, T. Hiraoki, K. Hikichi, T. Mikuni, M. Yazawa, K. Yagi, Nuclear magnetic resonance studies on calmodulin: calcium-induced conformational change, Biochemistry 22 (1983) 2573–2579.
[4] C.-L.A. Wang, A note on Ca^{2+} binding to calmodulin, Biochem. Biophys. Res. Commun. 130 (1985) 426–430.
[5] W.S. VanScyoc, B.R. Sorensen, E. Rusinova, W.R. Laws, J.B. Ross, M.A. Shea, Calcium binding to calmodulin mutants monitored by domain-specific intrinsic phenylalanine and tyrosine fluorescence, Biophys. J. 83 (2002) 2767–2780.
[6] J. Haiech, C.B. Klee, J.G. Demaille, Effects of cations on affinity of calmodulin for calcium: ordered binding of calcium ions allows the specific activation of calmodulin-stimulated enzymes, Biochemistry 20 (1981) 3890–3897.
[7] A. Crivici, M. Ikura, Molecular and structural basis of target recognition by calmodulin, Annu. Rev. Biophys. Biomol. Struct. 24 (1995) 85–116.
[8] Y. Saimi, C. Kung, Calmodulin as an ion-channel subunit, Annu. Rev. Physiol. 64 (2002) 289–311.
[9] T. Yuan, M.P. Walsh, C. Sutherland, H. Fabian, H.J. Vogel, Calcium-dependent and -independent interactions of the calmodulin-binding domain of cyclic nucleotide phosphodiesterase with calmodulin, Biochemistry 38 (1999) 1446–1455.
[10] T. Yuan, H.J. Vogel, C. Sutherland, M.P. Walsh, Characterization of the Ca^{2+}-dependent and -independent interactions between calmodulin and its binding domain of inducible nitric oxide synthase, FEBS Lett. 431 (1998) 210–214.
[11] E.O. Hernández, R. Trejo, A.M. Espinosa, A. González, A. Mújica, Calmodulin binding proteins in the membrane vesicles released during the acrosome reaction and in the perinuclear material in isolated acrosome reacted sperm heads, Tissue Cell 26 (1994) 849–865.
[12] B.R. Sorensen, J.T. Eppel, M.A. Shea, Paramecium calmodulin mutants defective in ion channel regulation associate with melittin in the absence of calcium but require it for tertiary collapse, Biochemistry 40 (2001) 896–903.
[13] C.L. Drum, S. Yan, J. Bard, Y. Shen, D. LU, S. Soelaiman, Z. Grabarek, A. Bohm, W. Tang, Structural basis for the activation of anthrax adenylyl cyclase exotoxin by calmodulin, Nature 415 (2002) 396–402.
[14] M.A. Schumacher, A.F. Rivard, H.P. Bachinger, J.P. Adelman, Structure of the gating domain of a Ca^{2+}-activated K^+ channel complexed with Ca^{2+}/calmodulin, Nature 410 (2001) 1120–1124.
[15] C.P. Moore, G. Rodney, J.Z. Zhang, L. Santacruz-Toloza, G. Strasburg, S.L. Hamilton, Apocalmodulin and Ca^{2+} calmodulin bind to the same region on the skeletal muscle Ca^{2+} release channel, Biochemistry 38 (1999) 8532–8537.
[16] G.G. Rodney, C.P. Moore, B.Y. Williams, J.Z. Zhang, J. Krol, S.E. Pedersen, S.L. Hamilton, Calcium binding to calmodulin leads to an N-terminal shift in its binding site on the ryanodine receptor, J. Biol. Chem. 276 (2001) 2069–2074.
[17] X. Huang, B. Fruen, D.T. Farrington, T. Wagenknecht, Z. Liu, Calmodulin-binding locations on the skeletal and cardiac ryanodine receptors, J. Biol. Chem. 287 (2012) 30328–30335.
[18] A. Tripathy, L. Xu, G. Mann, G. Meissner, Calmodulin activation and inhibition of skeletal muscle Ca^{2+} release channel (ryanodine receptor), Biophys. J. 69 (1995) 106–119.
[19] A.A. Maximciuc, J.A. Putkey, Y. Shamoo, K.R. Mackenzie, Complex of calmodulin with a ryanodine receptor target reveals a novel, flexible binding mode, Structure 14 (2006) 1547–1556.
[20] C.B. Boschek, H. Sun, D.J. Bigelow, T.C. Squier, Different conformational switches underlie the calmodulin-dependent modulation of calcium pumps and channels, Biochemistry 47 (2008) 1640–1651.
[21] C.P. Moore, J.Z. Zhang, S.L. Hamilton, A role for cysteine 3635 of RYR1 in redox modulation and calmodulin binding, J. Biol. Chem. 274 (1999) 36831–36834.
[22] N. Yamaguchi, C. Xin, G. Meissner, Identification of apocalmodulin and Ca^{2+}-calmodulin regulatory domain in skeletal muscle Ca^{2+} release channel, ryanodine receptor, J. Biol. Chem. 276 (2001) 22579–22585.
[23] N. Yamaguchi, L. Xu, D.A. Pasek, K.E. Evans, G. Meissner, Molecular basis of calmodulin binding to cardiac muscle Ca^{2+} release channel (ryanodine receptor), J. Biol. Chem. 278 (2003) 23480–23486.
[24] N. Yamaguchi, L. Xu, D.A. Pasek, K.E. Evans, S.R. Chen, G. Meissner, Calmodulin regulation and identification of calmodulin binding region of type-3 ryanodine receptor calcium release channel, Biochemistry 44 (2005) 15074–15081.
[25] M. Samsó, T. Wagenknecht, Apocalmodulin and Ca^{2+}-calmodulin bind to neighboring locations on the ryanodine receptor, J. Biol. Chem. 277 (2002) 1349–1353.
[26] L.W. Xiong, R.A. Newman, G.G. Rodney, O. Thomas, J.Z. Zhang, A. Persechini, M.A. Shea, S.L. Hamilton, Lobe-dependent regulation of ryanodine receptor type 1 by calmodulin, J. Biol. Chem. 277 (2002) 40862–40870.
[27] H. Zhang, J. Zhang, C.I. Danila, S.L. Hamilton, A noncontiguous, intersubunit binding site for calmodulin on the skeletal muscle Ca^{2+} release channel, 2782003. 8348–8355.
[28] C.B. Boschek, T.E. Jones, T.C. Squier, D.J. Bigelow, Calcium occupancy of N-terminal sites within calmodulin induces inhibition of the ryanodine receptor calcium release channel, Biochemistry 46 (2007) 10621–10628.
[29] S. Pedigo, M.A. Shea, Quantitative endoproteinase GluC footprinting of cooperative Ca^{2+} binding to calmodulin: proteolytic susceptibility of E31 and E87 indicates interdomain interactions, Biochemistry 34 (1995) 1179–1196.
[30] B.R. Sorensen, L.A. Faga, R. Hultman, M.A. Shea, Interdomain linker increases thermostability and decreases calcium affinity of calmodulin N-domain, Biochemistry 41 (2002) 15–20.
[31] B.R. Sorensen, M.A. Shea, Interactions between domains of apo calmodulin alter calcium binding and stability, Biochemistry 37 (1998) 4244–4253.
[32] W.S. VanScyoc, R.A. Newman, B.R. Sorensen, M.A. Shea, Calcium binding by calmodulin mutants having domain-specific effects on regulation of ion channels, Biochemistry 45 (2006) 14311–14324.
[33] J.A. Putkey, G.R. Slaughter, A.R. Means, Bacterial expression and characterization of proteins derived from the chicken calmodulin cDNA and a calmodulin processed gene, J. Biol. Chem. 260 (1985) 4704–4712.

[34] G.H. Beaven, E.R. Holiday, Ultraviolet absorption spectra of proteins and amino acids, Adv. Protein Chem. 7 (1952) 319–386.
[35] R.A. Newman, W.S. Van Scyoc, B.R. Sorensen, O.R. Jaren, M.A. Shea, Interdomain cooperativity of calmodulin to melittin preferentially increases calcium affinity of sites I and II, Proteins Struct. Funct. Bioinforma. 71 (2008) 1792–1812.
[36] T.I. Evans, M.A. Shea, Energetics of calmodulin domain interactions with the calmodulin binding domain of CaMKII, Proteins 76 (2009) 47–61.
[37] M.A. Shea, B.R. Sorensen, S. Pedigo, A. Verhoeven, Proteolytic footprinting titrations for estimating ligand-binding constants and detecting pathways of conformational switching of calmodulin, Methods Enzymol. 323 (2000) 254–301.
[38] G.S. Adair, The osmotic pressure of haemoglobin in the absence of salts, Containing Papers of a Mathematical and Physical Character, Proceedings of the Royal Society of London Series A, 109, 1925, pp. 292–300.
[39] M.L. Johnson, S.G. Frasier, Nonlinear least-squares analysis, Methods Enzymol. 117 (1985) 301–342.
[40] P.G. Richman, C.B. Klee, Specific perturbation by Ca^{2+} of tyrosyl residue 138 of calmodulin, J. Biol. Chem. 254 (1979) 5372–5376.
[41] R.E. Klevit, Spectroscopic analyses of calmodulin and its interactions, Methods Enzymol. 102 (1983) 82–104.
[42] R. Newman, Ph.D., University of Iowa (2006).
[43] B.R. Fruen, D.J. Black, R.A. Bloomquist, J.M. Bardy, J.D. Johnson, C.F. Louis, E.M. Balog, Regulation of the RYR1 and RYR2 Ca^{2+} release channel isoforms by Ca^{2+}-insensitive mutants of calmodulin, Biochemistry 42 (2003) 2740–2747.
[44] Z. Akyol, J.A. Bartos, M.A. Merrill, L.A. Faga, O.R. Jaren, M.A. Shea, J.W. Hell, Apo–calmodulin binds with its COOH-terminal domain to the N-methyl-D-aspartate receptor NR1 C0 region, J. Biol. Chem. 279 (2004) 2166–2175.
[45] N.T. Theoharis, B.R. Sorensen, J. Theisen-Toupal, M.A. Shea, The neuronal voltage-dependent sodium channel type II IQ motif lowers the calcium affinity of the C-domain of calmodulin, Biochemistry 47 (2008) 112–123.
[46] K. Lau, M.M. Chan, F. Van Petegem, Lobe-specific calmodulin binding to different ryanodine receptor isoforms, Biochemistry 53 (2014) 932–946.
[47] J. Trewhella, D.K. Blumenthal, D.K. Rokop, P.A. Seeger, Small-angle scattering studies show distinct conformations of calmodulin in its complexes with two peptides based on the regulatory domain of the catalytic subunit of phosphorylase kinase, Biochemistry 29 (1990) 9316–9324.
[48] M. Dasgupta, T. Honeycutt, D.K. Blumenthal, The gamma-subunit of skeletal muscle phosphorylase kinase contains two noncontiguous domains that act in concert to bind calmodulin, J. Biol. Chem. 264 (29) (1989) 17156–17163.
[49] T.S. Priddy, E.S. Price, C.K. Johnson, G.M. Carlson, Single molecule analyses of the conformational substates of calmodulin bound to the phosphorylase kinase complex, Protein Sci. 16 (2007) 1017–1023.
[50] T.I.A. Evans, M.A. Shea, Domain-specific calmodulin interactions with CaMKII, Biophys. J. (2006) 519a.
[51] P.M. Bayley, W.A. Findlay, S.R. Martin, Target recognition by calmodulin: dissecting the kinetics and affinity of interaction using short peptide sequences, Protein Sci. 5 (1996) 1215–1228.
[52] S. Ohki, U. Iwamoto, S. Aimoto, M. Yazawa, K. Hikichi, Mg^{2+} inhibits formation of $4Ca^{2+}$-calmodulin–enzyme complex at lower Ca^{2+} concentrations: ^{1}H and ^{113}Cd NMR studies, J. Biol. Chem. 268 (17) (1993) 12388–12392.
[53] S. Ohki, M. Ikura, M. Zhang, Identification of Mg^{2+}-binding sites and the role of Mg^{2+} on target recognition by calmodulin, Biochemistry 36 (1997) 4309–4316.
[54] S.R. Martin, L. Masino, P.M. Bayley, Enhancement by Mg^{2+} of domain specificity in Ca^{2+}-dependent interactions of calmodulin with target sequences, Protein Sci. 9 (2000) 2477–2488.
[55] J.J. Falke, S.K. Drake, A.L. Hazard, O.B. Peersen, Molecular tuning of ion binding to calcium signaling proteins, Q. Rev. Biophys. 27 (1994) 219–290.
[56] B. Wang, S.R. Martin, R.A. Newman, S.L. Hamilton, M.A. Shea, P.M. Bayley, K.M. Beckingham, Biochemical properties of V91G calmodulin: a calmodulin point mutation that deregulates muscle contraction in *Drosophila*, Protein Sci. 13 (2004) 3285–3297.
[57] B.R. Fruen, E.M. Balog, J. Schafer, F.R. Nitu, D.D. Thomas, R.L. Cornea, Direct detection of calmodulin tuning by ryanodine receptor channel targets using a Ca^{2+}-sensitive acrylodan-labeled calmodulin, Biochemistry 44 (2005) 278–284.
[58] J. Kim, S. Ghosh, H. Liu, M. Tateyama, R.S. Kass, G.S. Pitt, Calmodulin mediates Ca^{2+} sensitivity of sodium channels, J. Biol. Chem. 279 (2004) 45004–45012.
[59] T.S. Ulmer, S. Soelaiman, S. Li, C.B. Klee, W.J. Tang, A. Bax, Calcium dependence of the interaction between calmodulin and anthrax edema factor, J. Biol. Chem. 278 (2003) 29261–29266.
[60] O.B. Peersen, T.S. Madsen, J.J. Falke, Intermolecular tuning of calmodulin by target peptides and proteins: differential effects on Ca^{2+} binding and implications for kinase activation, Protein Sci. 6 (1997) 794–807.
[61] S.E. O'Donnell, L. Yu, C.A. Fowler, M.A. Shea, Recognition of beta-calcineurin by the domains of calmodulin: thermodynamic and structural evidence for distinct roles, Proteins 79 (2011) 765–786.
[62] M.J. Zhang, T. Yuan, J.M. Aramini, H.J. Vogel, Interaction of calmodulin with its binding domain of rat cerebellar nitric oxide synthase — a multinuclear NMR study, J. Biol. Chem. 270 (1995) 20901–20907.
[63] M. Ikura, N. Hasegawa, S. Aimoto, M. Yazawa, K. Yagi, K. Hikichi, ^{113}Cd-NMR evidence for cooperative interaction between amino- and carboxyl-terminal domains of calmodulin, Biochem. Biophys. Res. Commun. 161 (3) (1989) 1233–1238.
[64] G.K. Ackers, M.A. Shea, F.R. Smith, Free energy coupling within macromolecules: the chemical work of ligand binding at the individual sites in cooperative systems, J. Mol. Biol. 170 (1983) 223–242.
[65] L.S. Maier, M.T. Ziolo, J. Bossuyt, A. Persechini, R. Mestril, D.M. Bers, Dynamic changes in free Ca-calmodulin levels in adult cardiac myocytes, J. Mol. Cell. Cardiol. 41 (2006) 451–458.
[66] D.J. Black, Q.K. Tran, A. Persechini, Monitoring the total available calmodulin concentration in intact cells over the physiological range in free Ca^{2+}, Cell Calcium 35 (2004) 415–425.
[67] S. Kakiuchi, S. Yasuda, R. Yamazaki, Y. Teshima, K. Kanda, R. Kakiuchi, K. Sobue, Quantitative determinations of calmodulin in the supernatant and particulate fractions of mammalian tissues, J. Biochem. 92 (1982) 1041–1048.
[68] R.L. Cornea, F. Nitu, S. Gruber, K. Kohler, M. Satzer, D.D. Thomas, B.R. Fruen, FRET-based mapping of calmodulin bound to the RyR1 Ca^{2+} release channel, Proc. Natl. Acad. Sci. U. S. A. 106 (2009) 6128–6133.
[69] J.K. Kranz, E.K. Lee, A.C. Nairn, A.J. Wand, A direct test of the reductionist approach to structural studies of calmodulin activity: relevance of peptide models of target proteins, J. Biol. Chem. 277 (2002) 16351–16354.
[70] A.R. Penheiter, Z. Bajzer, A.G. Filoteo, R. Thorogate, K. Török, A.J. Caride, A model for the activation of plasma membrane calcium pump isoform4b by calmodulin, Biochemistry 42 (2003) 12115–12124.
[71] M. Dasgupta, D.K. Blumenthal, Characterization of the regulatory domain of the gamma-subunit of phosphorylase kinase — the two noncontiguous calmodulin-binding subdomains are also autoinhibitory, J. Biol. Chem. 270 (1995) 22283–22289.
[72] G.G. Rodney, B.Y. Williams, G.M. Strasburg, K. Beckingham, S.L. Hamilton, Regulation of RYR1 activity by Ca^{2+} and calmodulin, Biochemistry 39 (2000) 7807–7812.
[73] G.G. Rodney, J. Krol, B. Williams, K. Beckingham, S.L. Hamilton, The carboxy-terminal calcium binding sites of calmodulin control calmodulin's switch from an activator to an inhibitor of RYR1, Biochemistry 40 (2001) 12430–12435.
[74] L. Xiong, J. Zhang, R. He, S.L. Hamilton, A Ca^{2+}-binding domain in RyR1 that interacts with the calmodulin binding site and modulates channel activity, Biophys. J. 90 (2006) 173–182.
[75] P.J. Kraulis, *MOLSCRIPT*: a program to produce both detailed and schematic plots of protein structures, J. Appl. Crystallogr. 24 (1991) 946–950.
[76] E.A. Merritt, D.J. Bacon, Raster3D: photorealistic molecular graphics methods, Methods Enzymol. 277 (1997) 505–524.
[77] Y.S. Babu, C.E. Bugg, W.J. Cook, Structure of calmodulin refined at 2.2 Å resolution, J. Mol. Biol. 204 (1988) 191–204.